

On the impact of interference
from TDD terminal stations
to FDD terminal stations
in the 2.6 GHz band

Statement

Publication date:

21 April 2008

Contents

Section		Page
1	Executive summary	1
2	Introduction and overview	2
3	Radio characteristics of terminal stations relating to adjacent-channel interference	5
4	Evaluation of terminal-to-terminal interference	9
5	Conclusions and impact on adopted technical conditions and spectrum packaging	18
Annex		Page
1	Modelling methodology	20
2	Terminal station transmission characteristics	38
3	Terminal station receiver performance	44

Section 1

Executive summary

- 1.1 This document reports on a detailed study undertaken by Ofcom in order to investigate the impact of adjacent-channel interference from TDD terminal stations to FDD terminal stations in the 2.6 GHz band.
- 1.2 The analysis examines scenarios where a TDD cellular network and a FDD cellular network both serve the same geographical area, and where the TDD network operates within frequency blocks that are adjacent to those used by the FDD network in the downlink direction, thereby giving rise to the possibility of terminal-to-terminal interference. The terminal station densities considered are commensurate with those observed in busy *hot-spot* locations.
- 1.3 The impact of terminal-to-terminal interference on the downlink data throughput of a FDD terminal station is evaluated by taking account of interferer radiation masks, non-ideal receiver filter characteristics, non-linear effects at the receiver, and receiver saturation (or blocking). These features have been quantified based on the measured performance of a number of commercially available UTRA-FDD handsets in the 2.1 GHz band.
- 1.4 Moreover, we have used realistic models to characterise the behaviour of the terminal stations, including the operation of functions such as adaptive modulation and coding, power control, and scheduling (i.e., bursty transmissions).
- 1.5 The following conclusions are drawn from the results of this study:
 - There is little risk of 1st adjacent-block interference from TDD terminal stations towards FDD terminal stations when the former are served by pico-cellular base stations.
 - The impact of terminal-to-terminal interference from the 2nd adjacent-block or beyond (i.e., greater frequency offsets) is shown to be insignificant, even when the TDD terminal stations are served by macro-cellular base stations.
 - The results also broadly apply to the cases of interference from FDD terminal stations to TDD terminal stations, and to cases of interference between TDD terminal stations.
 - The adoption of restricted blocks – which is required to mitigate base-to-base interference at the relevant frequency boundaries – also provides the means for mitigation of terminal-to-terminal interference towards standard blocks. One implication of this result is that all standard blocks within a given category (i.e., paired or unpaired) have a similar potential for suffering from terminal-to-terminal interference.
 - The low potential for terminal-to-terminal interference in the 2.6 GHz band means that FDD terminals which are designed for operation in the band-plan specified in ECC Decision (05)05 will also work in other band-plans (i.e., different FDD/TDD splits) that are consistent with CEPT Report 19.

Section 2

Introduction and overview

- 2.1 As a result of its availability for mobile services in the EU and a number of countries worldwide, the 2.6 GHz band provides an important opportunity for the introduction of next generation mobile technologies as well as for the provision of additional capacity for networks using the current generation of technologies. There are two main competing technologies for the provision of mobile services at 2.6 GHz:
- i) WiMAX, developed with a strong input from the internet and IT sectors, which is optimised for data services (with voice over IP being one of the potential data applications) and for which equipment is ready and available now for use of unpaired spectrum through time division duplex (TDD) operation; and
 - ii) 3G mobile technologies which are in use now in the UK and, significantly, their likely successor technologies based on the LTE standard which is also optimised for data and is primarily (though not exclusively) based on use of paired spectrum through frequency division duplex (FDD) operation.
- 2.2 Given the requirement for provision of both paired and unpaired spectrum in the 2.6 GHz band, one can identify four types of inter-system adjacent-channel interference. These include:
- a) base station to terminal station interference;
 - b) terminal station to base station interference;
 - c) base station to base station interference; and
 - d) terminal station to terminal station interference.
- 2.3 Categories (a) and (b) above are no different from the types of interference which occur at the frequency boundaries which separate adjacent FDD cellular systems, or indeed, those which separate adjacent TDD cellular systems. Moreover, similar types of intra-system interference occur at the channel boundaries within any type of cellular system. Consequently, no special regulatory provisions for the mitigation of base-to-terminal or terminal-to-base adjacent-channel interference in the 2.6 GHz band are deemed to be necessary (other than those that are already embedded in the relevant technical standards in order to deal with such interference issues).
- 2.4 Categories (c) and (d) above, however, are specific to scenarios where transmissions in adjacent frequencies are subject to uplink and downlink phases which are not synchronised in time. This is characteristic across frequency boundaries which separate paired (FDD) and unpaired (TDD) spectrum, or across those which separate licensees of unpaired (TDD) spectrum where the uplink and downlink phases of the licensees are likely to be unsynchronised.
- 2.5 In this document we present an analysis of the interference caused by TDD terminal stations towards FDD terminal stations and its impact on FDD downlink throughput in the 2.6 GHz band. We specifically investigate the effects of interference in hot-spots, using realistic characterisations of terminal station behaviour.

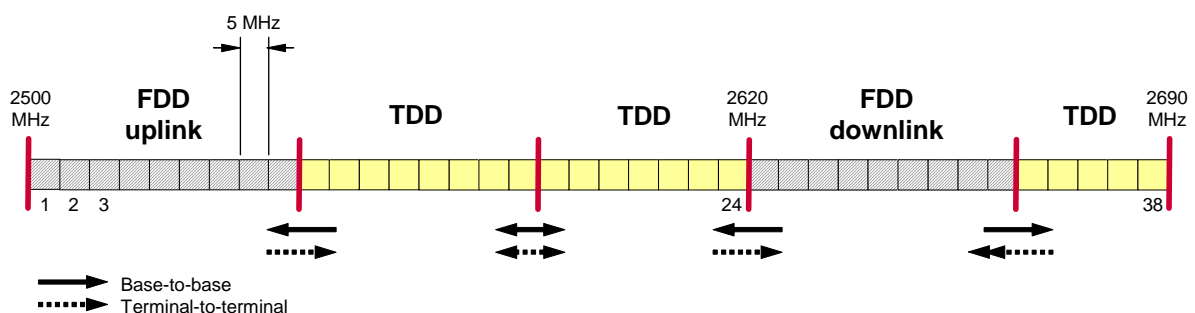
2.6 The analysis also:

- takes into account of the impact of adjacent-channel interferers in relation to a) radiation masks and non-ideal receiver filter characteristics, b) non-linear effects at the receiver, and c) receiver blocking (or saturation);
- examines the effects of interference in pico-cellular as well as in macro-cellular network deployments; and
- reflects the performance of commercially available UTRA-FDD user equipment, as derived through measurements commissioned by Ofcom¹, as opposed to the minimum requirements set out in the 3GPP Specifications (which were defined over 10 years ago).

2.7 Throughout this document, we refer to 5 MHz blocks (or channels) available in the 2.6 GHz band. Figure 1 identifies these blocks by numbering them from #1 (2500-2505 MHz) to #38 (2685-2690 MHz). Note that we use the terms “adjacent channel” and “adjacent block” interchangeably to refer to frequency blocks in the vicinity of a block of interest. Where we refer to the block immediately adjacent to a block of interest (i.e., where there is no frequency gap between the two blocks), we use the terms “1st adjacent channel” or “1st adjacent block”.

2.8 Figure 1 also illustrates the frequency boundaries in the 2.6 GHz band where base-to-base and terminal-to-terminal interference would occur for the example of a specific award outcome in which blocks #34 to #38 have, hypothetically, been won by TDD users as unpaired lots.

Figure 1: Frequencies at which base-to-base and terminal-to-terminal interference occur for an illustrative example of a specific award outcome.



2.9 Note that the nature of terminal-to-terminal interference is potentially different across the different boundaries illustrated in Figure 1. For example, there is a greater probability of TDD terminal stations which operate in the top end of the band (blocks #34 to #38 in the figure) to cause saturation (or blocking) of FDD terminal stations in the FDD downlink range. This is because standard FDD terminals made for the European marketplace are likely to have a front-end pass-band filter which allows through signals transmitted at all frequencies in the blocks #25 to #38. Hence, interference into FDD terminals from TDD terminals across this top boundary is likely to be greater than interference from TDD terminals operating from below block #24 where the pass-band filter should provide some attenuation. Meanwhile, the

¹ ERA Technology, “Measurements of UTRA-FDD user equipment characteristics in the 2.1 GHz band,” final report, April 2008. Document is available at: <http://www.ofcom.org.uk/consult/condocs/2ghzregsnotice/>.

interference into TDD terminals will depend on their filter characteristics and on whether adjacent TDD systems are synchronised or not; but, in principle, TDD terminals could receive interference from terminals of other FDD or non-synchronised TDD systems operating anywhere between block #1 and block #24.

- 2.10 In the sections that follow we present a detailed study of terminal-to-terminal adjacent-channel interference in the 2.6 GHz band:
- In Section 3 we provide an overview of the terminal station transceiver characteristics that are used in the analysis of terminal-to-terminal interference;
 - Section 4 contains a summary of the assumptions made in our analysis, and reports on the results of our evaluation of terminal-to-terminal interference;
 - In Section 5 we present a summary of our conclusions and explain the implications of the results of our analysis in the context of the technical conditions and spectrum packaging adopted by Ofcom for the 2.6 GHz band;
 - Annex 1 includes a detailed account of the methodology, modelling, and calculations used in our study of terminal-to-terminal interference. This is followed by Annexes 2 and 3, which report on the measured transceiver performance of a number of commercially available UTRA-FDD handsets in the 2.1 GHz band.
- 2.11 In the analysis reported in this document, we have taken full account of the work of the CEPT Working Group SE42, and the technical conditions recommended in CEPT Report 19², published in December 2007.

² “Report from CEPT to the European Commission in response to the Mandate to develop least restrictive technical conditions for frequency bands addressed in the context of WAPECS,” CEPT Report 19, December 2007.

Section 3

Radio characteristics of terminal stations relating to adjacent-channel interference

- 3.1 The scope for terminal-to-terminal adjacent-channel interference is driven by a mix of factors relating to:
- a) the experienced interference as a result of radiation spectral leakage and non-ideal receiver filter characteristics (i.e., limited ACIR);
 - b) third-order inter-modulation products, which represent the interference caused by non-linear behaviour at the receiver; and
 - c) saturation, or “blocking”, where a terminal station becomes overloaded by the high power levels of received adjacent-channel interferers which prevent the receiver from processing the wanted signal.
- 3.2 We consider below the way in which each of the above interference modes can most appropriately be characterised. In the process, we report on the measured¹ performance of commercially available UTRA-FDD user equipment. Parameters derived from these measurements (as opposed to the minimum requirements specified by 3GPP) are used in our further analysis of terminal-to-terminal interference. We note that our earlier technical work reported in the Discussion Document³ of August 2007 focused on the saturation (or blocking) effect caused by an interferer at the 3rd adjacent 5 MHz channel. In our new analysis we consider the impact of interference due to linear and non-linear receiver behaviour, as well as due to saturation, caused by interferers from a number of adjacent channels. The analysis is based on the use of 5 MHz channel widths as the component size in the spectrum packaging arrangements; however, as commented on later, the implications of the analysis also apply for systems using larger channel widths.

Adjacent-channel interference ratio

- 3.3 According to information theory, the maximum data throughput per unit bandwidth achievable over a communications link is a logarithmic function of the signal-to-interference-plus-noise ratio (SINR) experienced at the receiver. Consequently, the SINR is the key parameter in defining the spectral efficiency of a radio link. The level of SINR at a receiver is, in turn, a function of the radiated powers and spatial geometries of the transmitters of wanted and unwanted signals, in addition to the radio propagation environment.
- 3.4 Where an interferer transmits at a frequency that lies outside the nominal pass-band of the wanted signal, the level of interference experienced is a function of a) the interferer’s spectral leakage, as defined by its emission power spectral density, and b) the frequency response of the filtering at the receiver. These two effects can be characterised by the interferer’s adjacent-channel leakage ratio (ACLR) and the

³ Document “Award of available spectrum: 2500-2690MHz, 2010-2025MHz” is available at: <http://www.ofcom.org.uk/consult/condocs/2ghzdiscuss/main.pdf>.

receiver's adjacent-channel selectivity (ACS) respectively⁴. The combination of these two parameters, in the form of $(\text{ACLR}^{-1} + \text{ACS}^{-1})^{-1}$, represents the fraction of the received interferer power which is experienced as interference by the receiver, and is referred to as the adjacent-channel interference ratio (ACIR)⁵. In other words, for a received interferer power P_{AC} at frequency offset Δf from the wanted signal, and for an ACIR of $A(\Delta f)$, the experienced interference power is given by $P_i = P_{\text{AC}} / A(\Delta f)$.

- 3.5 Table 1 indicates the ACIRs for a terminal-to-terminal link with the interferer transmitting in the 1st to 4th adjacent 5 MHz blocks with respect to the wanted signal. These are computed based on the ACLR required for compliance with the corner points of the SE42 terminal station emission block-edge mask (BEM) adopted for the 2.6 GHz band (see Annex 2), and the measured filtering characteristics (i.e., ACS) of commercially available UTRA-FDD user equipment in the 2.1 GHz band (see Annex 3).

Table 1: Terminal-to-terminal ACIR, where the interfering terminal station just complies with SE42 BEMs when radiating at maximum in-block EIRP.

	nth adjacent block			
	n = 1	n = 2	n = 3	n = 4
ACLR (dB)	33	45	54	63
ACS (dB)	53	65	65	65
ACIR (dB)	33	45	53	61

- 3.6 The above ACIR values are applicable in circumstances where the interfering terminal station just complies with the BEM specifications when radiating at full power (i.e., an EIRP of 31 dBm). These ACIR values are dominated by the emission spectral leakage (ACLR) of the interferer.
- 3.7 However, we have developed separate ACIR values that apply when a terminal station radiates at less than full power. This is because spectral leakage typically reduces with respect to the in-block EIRP when a terminal station radiates at less than full power, thereby resulting in an improved ACLR, and consequently, improved ACIR. Measurements of commercially available UTRA-FDD user equipment in the 2.1 GHz band indicate that, for an EIRP of 20 dBm, the achieved ACLR is better than the minimum requirements specified in 3GPP TS 25.101 by around 8 dB at the 1st adjacent channel, by around 5 dB at the 2nd adjacent channel, and by more than 10 dB at greater frequency offsets (see Annex 2). Table 2 shows the improved ACIR values that apply, based on equivalent improvements in ACLR with respect to the SE42 BEMs, when the terminal station radiates at less than full power.

⁴ The ACLR of a signal is defined as the ratio of the signal's power (nominally equal to the power over the signal's pass-band) divided by the power of the signal when measured at the output of a (nominally rectangular) receiver filter centred on an adjacent frequency channel. The ACS of a receiver is defined as the ratio of the receiver's filter attenuation over its pass-band divided by the receiver's filter attenuation over an adjacent frequency channel. It can be readily shown that $\text{ACIR}^{-1} = \text{ACLR}^{-1} + \text{ACS}^{-1}$.

⁵ The ACIR is defined as the ratio of the power of an adjacent-channel interferer as received at the victim, divided by the interference power "experienced" by the victim receiver as a result of both transmitter and receiver imperfections.

Table 2: Terminal-to-terminal ACIR, where the interfering terminal station readily complies with SE42 BEMs when radiating at less than maximum in-block EIRP.

	nth adjacent block			
	n = 1	n = 2	n = 3	n = 4
ACLR (dB)	41	50	64	73
ACS (dB)	53	65	65	65
ACIR (dB)	40	50	61	64

3.8 The ACIRs values in Table 1 and Table 2 are used in our analysis of terminal-to-terminal interference when considering interference from standard blocks and restricted blocks respectively.

Third-order inter-modulation products

3.9 In addition to the effects discussed above, it is also possible for signals received at adjacent channels to result in interference through inter-modulation products caused by the non-linear behaviour of the receiver. Consider a wanted signal received in frequency block n_0 . Then, third-order nonlinearities in the behaviour of the receiver would imply that two interferers received at frequency blocks $n_0 + \Delta n$ and $n_0 + 2\Delta n$ can result in co-channel interference within frequency block n_0 .

3.10 These so-called inter-modulation (IM) products can be a significant source of degradation in SINR when the receiver is exposed to multiple un-attenuated adjacent-channel interferers. For example, a FDD terminal station receiving in block #34 would be subject to third-order IM products caused by TDD terminal station interferers received in block pairs (#35, #36) and (#36, #38). Similarly, a FDD terminal station receiving in block #25 would be subject to third-order IM products originating from block pairs (#23, #24), (#21, #23), and others⁶.

3.11 3GPP TS 25.101 specifies that the inter-modulation characteristics of a FDD terminal station receiver should be such that the reception of two interferers, each at a level of -46 dBm and at frequency offsets of 10 and 20 MHz from the wanted carrier, should at most result in a 3 dB desensitisation. Measurements commissioned by Ofcom suggest that commercially available UTRA-FDD user equipment in the 2.1 GHz band suffer from 3 dB desensitisation with interferers at power levels of around -30 dBm (see Annex 3). This latter result, which implies that actual terminals perform 16 dB better than the 3GPP minimum requirements, is used for the modelling of IM products in our analysis.

Receiver saturation (blocking)

3.12 Naturally, the components in a receiver chain are unable to deal with arbitrarily large signal levels. If the absolute values of the received adjacent-channel signals are beyond a certain threshold, the receiver will be overloaded or saturated. The performance of the receiver is difficult to model in such circumstances, and parameters (such as the ACIR) which model the normal operation of the receiver are no longer helpful in predicting the levels of interference experienced or the achievable throughputs. Our analysis assumes that the saturation of the receiver

⁶ Interferers at lower frequency blocks would be increasingly attenuated by the FDD terminal station's front-end (duplex) filter.

would result in a zero radio link throughput. This is a conservative assumption, as in practice it is unlikely that throughput would fall to zero in all cases.

- 3.13 3GPP TS 25.101 specifies that a UTRA-FDD terminal station receiver should be able to apply a linear ACS of 33 dB to a 1st adjacent-channel interferer received at a power level of up to –25 dBm. Measurements commissioned by Ofcom suggest that commercially available UTRA-FDD user equipment in the 2.1 GHz band perform much better than this and can apply an ACS of 33 dB when subjected to a 1st adjacent-channel interferer power of up to –10 dBm or greater⁷, i.e., 15 dB better than the 3GPP minimum requirements (see Annex 3). Measurements indicate that even greater interferer power levels can be supported at the 2nd and 3rd adjacent channels. A threshold of –10 dBm is used in our modelling of saturation effects; i.e., if the aggregate received power of the adjacent-channel interferers exceeds this threshold then the terminal station is assumed to suffer from saturation and the downlink throughput is assumed to drop to zero.

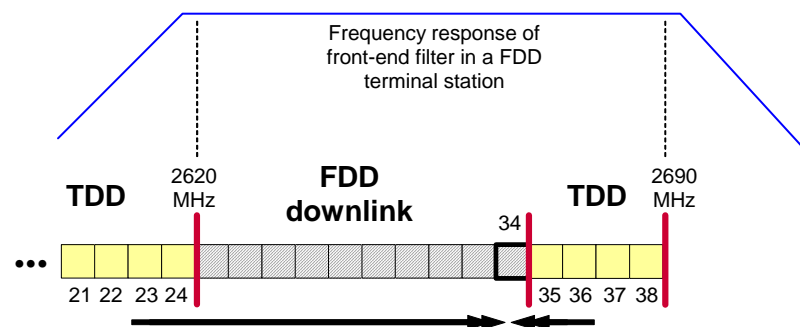
⁷ Furthermore, measurements indicate that an ACS of around 53 dB applies when the power of the adjacent-channel interferer is –20 dBm.

Section 4

Evaluation of terminal-to-terminal interference

4.1 In this section we summarise the results of our evaluation of the impact of interference caused by TDD terminal stations on the statistics of downlink throughput in a FDD cellular system. We consider the scenario where a TDD cellular network is deployed in the same geographical area as a FDD cellular network. We further assume that the TDD network operates within frequency blocks that are adjacent to those used by the FDD network in the downlink direction, thereby giving rise to the possibility of terminal-to-terminal interference. Figure 2 illustrates a specific award outcome and the sources of interference towards the paired (FDD) block #34 as examined in this study. We focus on block #34 since this is the FDD block that will be most susceptible to interference in this example. Note that this example corresponds to a total of 18 unpaired (TDD) blocks in the 2.6 GHz band.

Figure 2: Sources of terminal-to-terminal interference for the illustrative example of a specific award outcome. Arrows indicate direction of potential terminal-to-terminal interference into block #34.



4.2 It should be pointed out that, in the context of terminal-to-terminal interference towards FDD mobile stations, there is a greater risk of IM products and saturation from adjacent-channel interferers received in blocks #25 to #38, than there is from those received in blocks #24 and below. This is because interferers received in blocks #25 to #38 fall within the pass-band of a FDD terminal station's front-end (duplex) filter, and would therefore not be attenuated prior to amplification and further processing. As shown in Figure 2, the pass-band of the front-end filter would nominally cover the frequency range 2620 MHz to 2690 MHz in order to allow the terminal station to receive signals from base stations transmitting in any of the paired (FDD) downlink blocks⁸. Interferers received in blocks #24 and below, however, would fall outside the filter's pass-band and would therefore be attenuated according to their frequency offsets from the pass-band edge. In the modelling of inter-modulation and blocking, we account for the roll-off of the front-end filter via attenuations of 0, 4, 8, and 12 dB at blocks #24, #23, #22, and #21 respectively.

⁸ While the use of tuneable front-end filters could in principle mitigate against adjacent-channel interferers in blocks #25 to #38, we do not envisage that such technologies can be cost-effectively incorporated within terminal stations in the near future.

- 4.3 The TDD system is modelled based on physical layer parameters that are similar to those of WiMAX⁹ (see Annex 1). Each TDD terminal station is scheduled for uplink transmission by its serving base station and is allocated the appropriate frequency and time resource in accordance with the throughput required by the service and the throughput achievable on the radio link. The latter is a function of uplink EIRP, propagation path-loss and shadowing, and interference. The model includes uplink intra-system interference from a ring of adjacent TDD cells.
- 4.4 The FDD system is modelled based on physical layer parameters that are similar to those of UTRA-FDD HSDPA¹⁰ (see Annex 1). Here the metric of interest is the statistics of downlink throughput over the cell area as a result of a FDD terminal station receiving one packet per scheduling interval from its serving base station. The FDD downlink throughput is a function of downlink EIRP, propagation path-loss and shadowing, and interference. The model includes downlink intra-system interference from a ring of adjacent FDD cells.
- 4.5 The extended (urban) Hata model¹¹ is used to characterise mean path-loss over all radio links, assuming antenna heights of 30 and 1.5 metres for base stations and terminal stations respectively¹².
- 4.6 The impact of terminal-to-terminal interference on the FDD downlink is strongly dictated by the bursty natures of both TDD terminal station transmissions and FDD terminal station receptions. These effects are captured by a) modelling uplink scheduling of TDD packets, with those requiring least resources scheduled first, and b) assuming a FDD downlink packet arrival time that is uniformly distributed over the scheduling interval.
- 4.7 It should be pointed out that collisions between uplink TDD packets and a FDD downlink packet received at a FDD terminal station need not necessarily have a severe impact on the FDD downlink throughput. The effects of such collisions depend on the number of TDD transmitters, the amount of time-frequency resource utilised by each TDD packet transmission and their degrees of overlap (in time) with the FDD packet, the EIRP of the TDD terminal stations, and their spatial separations from the FDD terminal station.
- 4.8 The above effects are captured via Monte Carlo simulations modelling the urban macro-cellular scenario depicted in Figure 3.

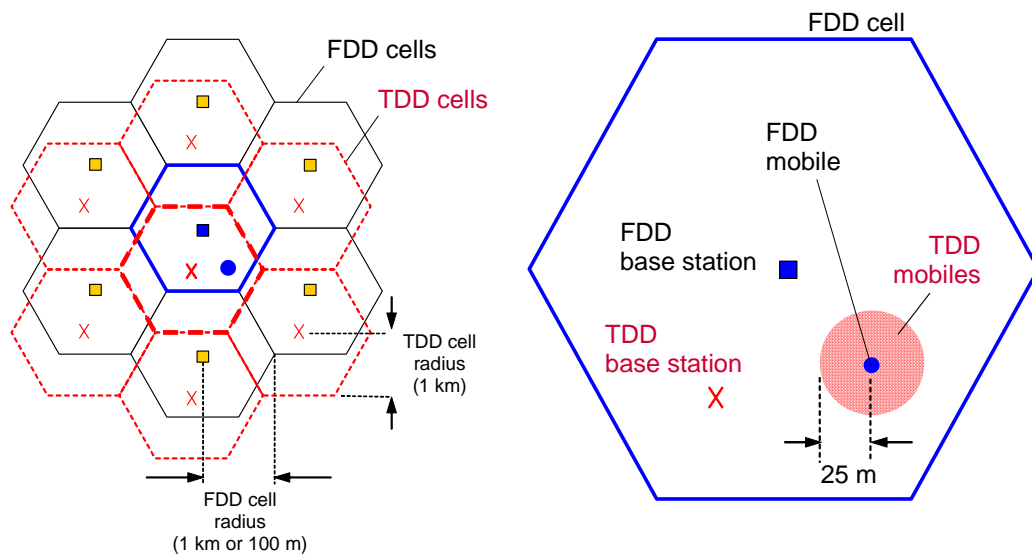
⁹ The TDD system is modelled with a nominal channel bandwidth of 4.1 MHz, uplink/downlink ratio of 1:3, frame duration of 5 ms, uplink sub-frame duration of 1.25 ms, scheduling interval of 20 ms, and adaptive modulation and coding (up to 64-QAM, ¾ rate coding) with power control. A throughput of 75% of the Shannon Limit is assumed over the radio link. It is assumed that VOIP and video conferencing services require throughputs of 30 kbits/s and 360 kbits/s respectively.

¹⁰ The FDD system is modelled with a nominal channel bandwidth of 3.84 MHz, downlink packet duration of 2 ms, scheduling interval of 20 ms, and adaptive modulation and coding (up to 16-QAM, ¾ rate coding). A throughput of 75% of the Shannon Limit is assumed over the radio link.

¹¹ European Radiocommunications Office, "SEAMCAT user manual (Software version 2.1)," February 2004.

¹² For all base-terminal links, shadowing standard deviations of 3.5 dB and 12 dB are assumed for separations of less than 40 metres and greater than 40 metres respectively. For terminal-to-terminal links, the propagation model corresponds to free-space path-loss (propagation exponent of 2) and a shadowing standard deviation of 3.5 dB. This represents line-of-sight propagation in large open areas.

Figure 3: Urban macro-cellular FDD scenario.



- 4.9 In each Monte Carlo trial, the target FDD terminal station is randomly placed within the central FDD cell. A number of TDD terminal stations are then randomly distributed within a 25 metre radius of the FDD terminal station. Finally, the FDD terminal station (along with the surrounding TDD terminal stations) is randomly placed within a serving TDD cell. Note that this formulation corresponds to the case where the FDD terminal station is always in the proximity of a high density of TDD terminal stations (i.e., a TDD hot-spot). All terminal station locations are subject to a uniform probability density function. A FDD cell radius of 1 km is considered with maximum mean EIRPs of 61 dBm/(5 MHz) (antenna gain of 17 dBi) and 31 dBm/(5 MHz) (antenna gain of 0 dBi) for the FDD base stations and FDD terminal stations respectively.
- 4.10 In light of the findings of earlier work reported in the Discussion Document³ of August 2007, we have focused our further analysis on hot-spot scenarios only. In the representative hot-spot scenario examined here, the number of TDD terminal stations simulated is derived by reference to an average spatial density of 1 person per square-metre. This figure is consistent with measurements commissioned by Ofcom of population densities observed in hot-spot locations such as cafes and conference centres. We then assume that 1 in 10 individuals, randomly selected within the hot-spot, will be using their wireless device at any Monte-Carlo snapshot. Note that this still corresponds to a substantial number of 196 terminal stations simultaneously operating (although not necessarily simultaneously transmitting) within a radius of 25 metres from a potential victim of terminal-to-terminal interference. For this scenario we make what we consider to be the reasonable assumptions that 50% of the population use wireless equipment operating in bands other than the 2.6 GHz band, and that, of those who do use the 2.6 GHz band, only 50% use TDD technology.
- 4.11 The above assumptions imply that the spatial density of TDD terminal stations operating in the 2.6 GHz band at any Monte-Carlo snapshot would be of the order of 1/40 per square-metre. Given the total of 18 unpaired (TDD) blocks in the band-plan example considered (see Figure 2), and assuming a uniform distribution of TDD terminals across the blocks, the above corresponds to a density of 1/720 per square-metre per 5 MHz TDD block.

- 4.12 We first consider the situation where the TDD hot-spot is served by macro-cells supporting services in blocks #35¹³ to #38, and #21 to #24. A TDD cell radius of 1 km is considered, with a TDD base station receive antenna gain of 17 dBi, and a TDD terminal station maximum mean EIRP of 31 dBm/(5 MHz). We also use the ACIR values which were presented in Table 1.
- 4.13 Figure 4 shows the resulting cumulative probability distributions of the signal powers present at the output of the front-end filter of a FDD terminal station over the time interval in which a FDD downlink packet is received in block #34. As noted earlier, the adjacent-channel transmissions by TDD mobile stations in blocks #35 to #38 fall within the pass-band of the FDD mobile station's front-end filter, and so are unattenuated (thin solid lines). In comparison, the adjacent-channel transmissions by TDD mobile stations in blocks #21 to #24 fall outside the pass-band of the FDD terminal station's front-end filter, and so are attenuated in accordance with their respective frequency offsets from the pass-band edge (thin dashed lines). The thick dashed line corresponds to the aggregate (sum) of the received adjacent-channel interferer powers from TDD terminal station transmissions in blocks #21 to #24, and #34 to #38¹⁴. As can be seen, while the aggregate interferer power exceeds -25 dBm with a probability of around 10%, it does not exceed the -10 dBm saturation threshold of commercially available 3G user equipment. This implies that the probability of blocking is very low, even in hot-spot situations, and is likely to be even less of a problem than was indicated in the Discussion Document of August 2007.
- 4.14 The impact of the adjacent-channel interferers on the FDD downlink throughput is shown in Figure 5, again expressed in the form of cumulative probability distributions. The throughput distributions are shown both in the absence and presence of interference from TDD terminal station transmissions in adjacent blocks #35 to #38, and in blocks #21 to #24. Note that the throughputs correspond to a single 2 ms packet received over a 20 ms scheduling interval.
- 4.15 Note that the simulation results are not particularly sensitive to the throughputs required by the TDD services¹⁵. This is because, while a TDD mobile station which supports a high-rate service would require a greater fraction of the uplink radio resource, fewer such mobiles can be scheduled within a cell. The net effect is that aggregate interference generated remains broadly unchanged.

¹³ Note that block #35, itself, will be a restricted block for base station use as discussed in Ofcom's Statement of April 2008. However, in order to help illustrate the interference effects we assume, hypothetically, that it could be used for macro cells. The implications of making block #35 a restricted block will be considered later.

¹⁴ Note that it is the aggregate (sum) of the received adjacent-channel interferer powers from TDD terminal station transmissions which is relevant when considering the potential for saturation to occur. As can be seen, this total unwanted received power (thick dashed line in Figure 4) is significantly greater than the wanted received power in block #34 (thick solid line in Figure 4). However, the FDD terminal receiver will be tuned to block #34 and, provided it has not been saturated, will discriminate between the wanted and unwanted signals by suppressing the adjacent channel interferers through various stages of (intermediate-frequency and baseband) channel filtering.

¹⁵ TDD mobile stations are assumed to be accessing a VOIP service which requires a throughput of 30 kbits/s within a 20 ms scheduling interval.

Figure 4: Cumulative probability distributions of signal powers received at a FDD terminal station operating in block #34, in an urban macro-cellular FDD scenario, and in the presence of adjacent-channel TDD macro-cells.

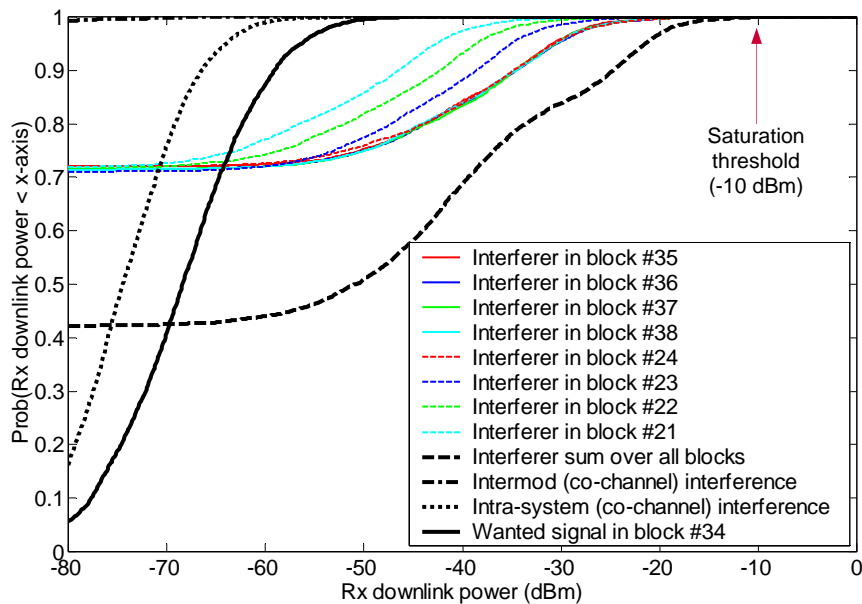
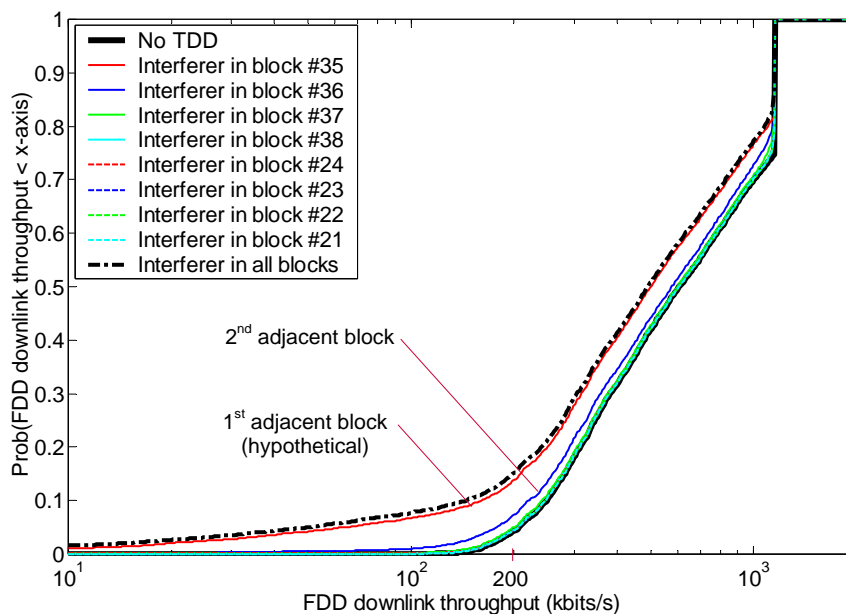


Figure 5: Cumulative probability distributions of FDD downlink throughput in block #34, in an urban macro-cellular FDD scenario, and in the presence of adjacent-channel TDD macro-cells.



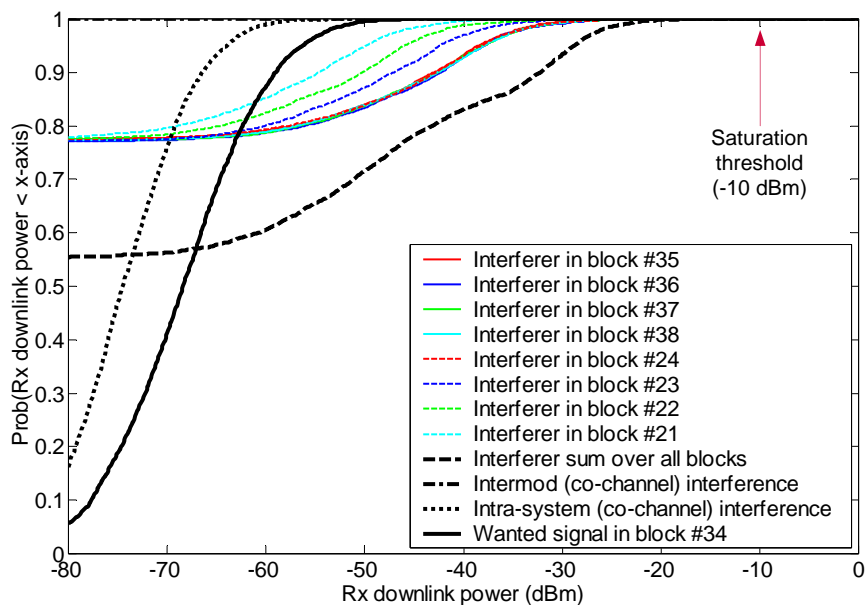
4.16 Figure 5 shows that, in the absence of interference from TDD terminal stations (thick solid curve), there is a 5% probability that the FDD downlink throughput drops below 205 kbits/s over the cell area. However, when in the proximity of TDD terminal stations transmitting in all the simulated adjacent blocks (thick dashed line), there is a 5% probability that the throughput drops below 55 kbits/s over the cell area.

- 4.17 An important point to note is that TDD terminal station transmissions in the 1st adjacent block, #35, contribute virtually all of the aggregate interference experienced by the FDD terminal station from TDD terminals (i.e., the additional impact of blocks #36 to #38 and #21 to #24 is negligible). When in the proximity of TDD terminal stations transmitting in the 2nd adjacent block #36 (but not the 1st adjacent block #35), there is a 5% probability that the throughput drops below 180 kbits/s over the cell area.
- 4.18 Based on the above results, we can draw the following conclusions.
- i) TDD terminal stations operating in the 2nd adjacent block (and beyond) with respect to a FDD terminal station cause little degradation in the FDD downlink throughput. The ACIR of 45 dB at the 2nd adjacent block is sufficient to mitigate the impact of terminal-to-terminal interference.
 - ii) TDD terminal stations operating in the 1st adjacent block with respect to a FDD terminal station can cause a significant (albeit graceful) degradation in throughput. The ACIR of only 33 dB at the 1st adjacent block is not sufficient to mitigate the impact of terminal-to-terminal adjacent-channel interference in the challenging geometries examined. However, this assumes that the 1st adjacent block is used for macro-cells, a point which we pick up below. But even so, this scenario would not represent a step change in performance experienced by FDD users.
 - iii) In principle, saturation of the FDD terminal station receiver can result in a severe (i.e., non-graceful) degradation in FDD downlink throughput. However, even in the challenging geometries investigated, the total received adjacent-channel interferer power is well below the -10 dBm threshold (see Figure 4) supported by 2.1 GHz UTRA-FDD user equipment commercially available today. This means that FDD terminal stations in the 2.6 GHz band, with receiver characteristics identical to (or better than) those that are available today in other bands, would be able to operate in the presence of TDD terminal stations without suffering from saturation. Consequently, one may conclude that saturation (or blocking) is not a material cause of throughput degradation in the context of terminal-to-terminal interference¹⁶.
 - iv) Third-order inter-modulation products were found to cause little degradation in downlink throughput in the scenarios investigated. This is because the received powers of any two adjacent-channel interferers rarely jointly exceed the threshold of -30 dBm (see Figure 4) supported by 2.1 GHz UTRA-FDD user equipment commercially available today.
- 4.19 Once again, we point out that the results apply to a scenario where a high-density of interfering TDD terminal stations is always present within a 25 metre radius of the FDD terminal station. This is clearly not always (or often) the case in practice, but the scenario is indicative of FDD downlink performance in the vicinity of TDD hot-spots.

¹⁶ Note that even in the unlikely event that terminal-to-terminal saturation effects were to cause material degradations in downlink throughput, such degradations would be observed equally in all FDD downlink blocks. This is because terminal station receiver components that are most likely to be saturated as a result of adjacent-channel interferers are typically protected only by a front-end RF filter whose pass-band covers the whole of the FDD downlink spectrum. An important implication of this is that, so far as saturation is concerned, all FDD downlink blocks in the 2.6 GHz band would have a similar usability.

- 4.20 Points i) and ii) above suggest that it is only the 1st adjacent-block terminal-to-terminal interference that could, hypothetically, be an issue in urban macro-cellular deployments.
- 4.21 In practice, of course, the unpaired (TDD) blocks immediately adjacent to paired (FDD) downlink blocks will be subject to restrictions on the base station in-block EIRP levels for reasons of mitigating base-to-base interference (as discussed in Ofcom’s Statement¹⁷ of April 2008). Hence, it is likely that these restricted blocks could only be used for deployment of TDD pico-cells. Moreover, in those situations where high densities of users are anticipated (e.g., conference centres, train stations, etc.) it is likely that operators of TDD networks would in any case want to deploy pico-cells in order to adequately satisfy the demands for throughput.
- 4.22 We have therefore taken the analysis further to examine the impact of interference caused by TDD pico-cellular deployments in restricted blocks where the TDD base stations are subject to a maximum in-block mean EIRP of 25 dBm/(5 MHz)¹⁸. Figure 6 and Figure 7 show the impact of TDD interference in this case, for a TDD cell radius of 100 metres. A TDD terminal station maximum in-block mean EIRP of 25 dBm/(5 MHz) is assumed in order to match that of the serving TDD base station. The ACIR values of Table 2 are also assumed here, corresponding to the higher ACLR values achieved by TDD terminal stations when transmitting below the maximum in-block mean EIRP of 31 dBm (e.g., when located within a pico-cell).

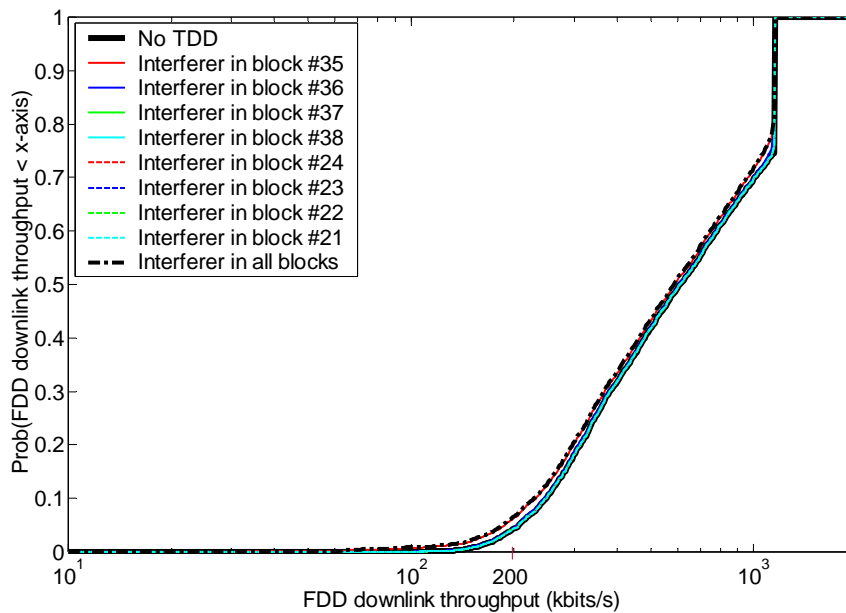
Figure 6: Cumulative probability distributions of signal powers received at a FDD terminal station operating in block #34, in an urban macro-cellular FDD scenario, and in the presence of TDD pico-cells.



¹⁷ Document “Award of available spectrum: 2500-2690 MHz, 2010-2025 MHz” is available at available at: <http://www.ofcom.org.uk/consult/condocs/2ghzregsnotice/>.

¹⁸ For computational simplicity, the analysis assumes pico-cellular TDD deployment in all adjacent blocks. However, as shown earlier, the effects of the 2nd adjacent block (and beyond) are very small even for macro-cellular TDD deployments, and so the results are not distorted by this assumption.

Figure 7: Cumulative probability distributions of FDD downlink throughput in block #34, in an urban macro-cellular FDD scenario, and in the presence of adjacent-channel TDD pico-cells



- 4.23 The results of Figure 7 clearly indicate that, when served by a TDD pico-cell, TDD terminal stations operating in a restricted 1st adjacent block with respect to a FDD terminal station cause little or no degradation in the FDD downlink throughput. There are two reasons for this. The first reason is that, due to its proximity to a serving base station, a TDD terminal can use high-order modulation and coding to achieve the required throughput without the need to use high transmission powers and large proportions of the uplink time-frequency resource. Secondly, the ACLR of the TDD terminal station (and hence the ACIR) improves as a result of the reduced in-block radiation power that applies in a pico-cell, thereby helping to further mitigate the impact of interference at the FDD terminal station.
- 4.24 The results of this further analysis confirm the substance of the conclusions that we presented in the Discussion Document of August 2007, namely that the effects of terminal-to-terminal interference are very modest. We have probed much further into the one area where there were residual concerns relating to hot-spot scenarios, and we have confirmed that the impact of interference is likely to be very limited even in these situations, particularly when taking account of measures such as the use of pico-cells. In carrying out this further analysis we have taken into account of interference experienced as a result of limited ACIR, inter-modulation products, and saturation effects, as requested by some respondents to the Discussion Document. Indeed, the results suggest that the chances of saturation (or blocking) are actually much smaller than even the earlier analysis had implied might be the case, and that the blocking effect is, in fact, smaller than that due to limited ACIR.
- 4.25 The main reasons why our further analysis indicates that the chances of blocking are even less than suggested in our earlier analysis are as follows.
- a) The measurements of commercially available FDD user equipment indicate that these perform significantly better than the minimum requirements set out in the 3GPP Specifications (which are now over 10 years old).

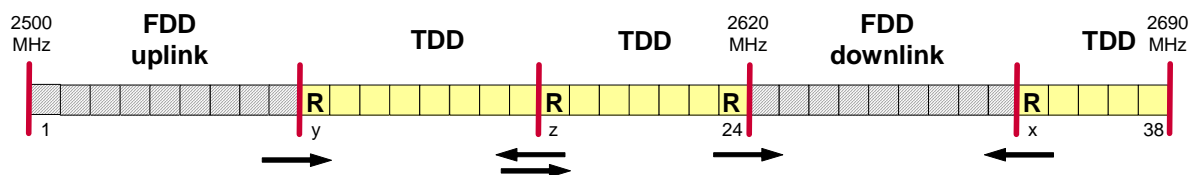
- b) We had used a simplified model in our previous work, whereby unwanted adjacent-channel signals received at a level above a pessimistic threshold value would automatically cause blocking of a FDD terminal station and result in a zero downlink throughput. We have now implemented a more realistic model, whereby the FDD terminal stations experience a more graceful degradation in performance (or drop in throughput) when adjacent-channel signal levels are below the threshold at which commercially available user equipment are found to suffer from blocking.
 - c) We have used more realistic models of both power control and uplink scheduling (i.e., bursty transmissions) for the TDD terminal stations. This also contributes to the reduced levels of interference experienced by FDD terminal stations. These are particularly noticeable in the case of TDD pico-cells which are likely to be deployed in locations where dense usage is anticipated.
- 4.26 Whilst this further analysis has focused on hot-spot scenarios, we can infer that the effects of interference in average density scenarios are also likely to be less than we had indicated in the Discussion Document of August 2007.
- 4.27 Although we have not explicitly evaluated the impact of interference on the quality of specific wireless services, our analysis suggests that any degradation in the achievable downlink packet throughput would be at most marginal, and that the resulting quality of services would be broadly the same as that achievable in the absence of terminal-to-terminal adjacent-channel interference.
- 4.28 Throughout our quantitative analysis we have focussed on the case of interference from TDD terminal stations to FDD terminal stations. However, as noted in paragraph 2.9, TDD terminal stations are similarly exposed to the effects of interference from terminal stations (and possibly more so given the number of blocks in which FDD and unsynchronised TDD terminals could transmit and which may fall within the front-end filter pass-band of TDD terminals).
- 4.29 Finally, we note that the presented analysis was undertaken for the case of FDD and TDD technologies using nominal channel bandwidths of 5 MHz. However, the results would still broadly apply in the case of greater channel bandwidths. This is because we have accounted for interferers from multiple adjacent 5 MHz blocks in our analysis which, to a first order, will be equivalent to interferers from a smaller number of wider blocks.

Section 5

Conclusions and impact on adopted technical conditions and spectrum packaging

- 5.1 As explained in Ofcom's Statement¹⁷ of April 2008, in order to adequately manage the risk of base-to-base interference, restricted 5 MHz blocks are applied at frequency boundaries which separate paired (FDD) and unpaired (TDD) spectrum, or at those which separate licensees of unpaired (TDD) spectrum.
- 5.2 For reference, the positions of the restricted blocks are repeated in Figure 8 below for the illustrative example of a specific award outcome. Although the restricted blocks are primarily intended to mitigate base-to-base interference, they also have important implications with respect to terminal-to-terminal interference, as discussed next.

Figure 8: Restricted blocks for the illustrative example of a specific award outcome. Arrows indicate direction of potential terminal-to-terminal interference. Restricted blocks are marked with "R".



- 5.3 Based on the results of the analysis outlined in the previous section, we believe that there is a risk of significant 1st adjacent-block interference from TDD terminal stations towards FDD terminal stations, where the TDD terminal stations are served by high-power macro-cellular base stations, and where there is a high density of TDD terminal stations operating in the spatial vicinity of the FDD terminal stations. However, even in such challenging scenarios, the impact of interference from TDD terminal stations operating in the 2nd adjacent block (or beyond) is insignificant. With reference to Figure 8, the above implies that there is little risk of interference toward FDD terminal stations from TDD terminal stations which operate in standard blocks.
- 5.4 The results further indicate that there is little risk of adjacent-block interference from TDD terminal stations towards FDD terminal stations if the former are served by low-power pico-cellular base stations. This is consistent with the case of TDD terminal stations that operate in the restricted blocks immediately below and above the FDD downlink spectrum (i.e., block #24 and block "x" in Figure 8). In other words, the restrictions on in-block EIRP imposed on TDD base stations in the aforementioned two restricted blocks remove the circumstances in which FDD terminal stations might suffer from interference caused by TDD terminal stations.
- 5.5 While in our analysis we specifically addressed the case of interference from TDD terminal stations to FDD terminal stations, the arguments and results also broadly apply in the opposite direction. This suggests that there is a risk of significant interference being experienced by TDD terminal stations operating in the restricted block above the FDD uplink band (i.e., block "y" in Figure 8) due to FDD terminal transmissions in the 1st adjacent block.

- 5.6 Extrapolating the results to the case of interference between unsynchronised TDD terminal stations, one may similarly conclude that the restricted blocks at the frequencies separating licensees of unpaired (TDD) spectrum (e.g., block “z” in Figure 8) effectively mitigate the impact of terminal-to-terminal interference toward TDD terminal stations in standard blocks, while TDD terminal stations in the restricted blocks are likely to suffer from terminal-to-terminal interference. It should be noted that here the licensees have the additional option of synchronising their uplink and downlink phases in order to effectively eliminate the possibility of terminal-to-terminal interference.
- 5.7 On the basis of the above analysis it is clear that the mitigation of terminal-to-terminal interference in standard blocks is already accommodated in the spectrum packaging illustrated in Figure 8 by the requirements imposed to manage base-to-base interference (see Ofcom’s Statement of April 2008). Consequently, no modification to the defined technical conditions or spectrum packaging is necessary to deal with additional terminal-to-terminal interference.
- 5.8 It is also important to note that, on the basis of the adopted technical conditions and spectrum packaging, the restricted blocks are not protected from terminal-to-terminal interference to the same extent as standard blocks. In other words, the usability of restricted blocks is defined by their limited protection from terminal-to-terminal interference as well as by the restrictions on base stations transmission rights.
- 5.9 The technical conditions adopted by Ofcom in relation to the use of the 2.6 GHz band by terminal stations are in line with those developed by the SE42 project team and are briefly presented below (see Ofcom’s Statement and Information Memorandum¹⁹ of April 2008 for further details).
- i) A terminal station in-block mean total radiated power (TRP) of 31 dBm/(5 MHz) will apply for all frequency blocks. For omni-directional transmissions, the specified TRP is equivalent to a mean EIRP of 31 dBm/(5 MHz), but allows the possibility of increased EIRP in specific directions subject to appropriate reductions of EIRP in other directions.
 - ii) All terminal station types will be subject to a single BEM profile, as detailed in Annex 2 of this document. This BEM is derived from the 3GPP TS 25.101 user equipment spectrum emission mask (relative) requirements based on a transmission power of 30 dBm/(3.84 MHz).

¹⁹ Document “Auction of spectrum: 2500–2690MHz, 2010–2025MHz” is available at: <http://www.ofcom.org.uk/consult/condocs/2ghzregsnotice/>.

Annex 1

Modelling methodology

Introduction

- A1.1 In this annex we present a detailed quantitative description of the modelling methodology and assumptions used in our analysis of adjacent-channel interference from TDD terminal stations to FDD terminal stations in the 2.6 GHz band. This is intended to complement the qualitative descriptions presented in Section 4 of this document.
- A1.2 We first explain the model used for the operation of the TDD uplink. This includes features such as adaptive modulation and coding, power control, and scheduling of TDD terminal station transmissions. Co-channel uplink interference from a ring of adjacent cells within the TDD system is also accounted for in this modelling.
- A1.3 We then describe the model used for quantifying the impact of terminal-to-terminal interference on a FDD terminal station. Here, we again assume the use of adaptive modulation and coding on the FDD downlink, and evaluate the levels of adjacent-channel interferer powers received based on the extent of time overlap between uplink TDD packets and downlink FDD packets. Co-channel downlink interference from a ring of adjacent cells within the FDD system is also accounted for in this modelling.
- A1.4 We subsequently show how the degradation in the FDD downlink SINR (and hence throughput) can be calculated as a function of the adjacent-channel interferer powers. This is performed by modelling the impact of a) adjacent-channel interference ratio (ACIR), b) receiver saturation, and c) inter-modulation products.
- A1.5 This annex ends with a description of the propagation models used in the analysis, and a list of parameter values assumed in the derivation of the results presented in Section 4 of this document. Note that we use WiMAX and UTRA-HSDPA as templates for the TDD and FDD technologies respectively.

Modelling of the TDD uplink

- A1.6 The results presented in Section 4 of this document quantify the impact of adjacent-channel interference originating from a number of TDD terminal stations radiating in frequency blocks #35 to #38 and #21 to #24, and located within a 25 m radius of a FDD terminal station tuned to receive in block #34.
- A1.7 In this sub-section, we describe in detail the methodology employed for the modelling of the above TDD terminal station transmissions. Note that the calculations presented apply to each of the TDD frequency blocks under investigation.

a) Adaptive modulation and coding in the TDD uplink

- A1.8 Modern radio access technologies invariably use adaptive modulation and coding (AMC), whereby the employed modulation order and forward error correction (FEC) coding rate are dynamically modified by the transmitter in response to variations in signal-to-interference-plus-noise ratio (SINR) at the receiver. This enables the

transmitter to maximise its utilisation of the capacity offered by the radio link at any given instant in time.

A1.9 In this study, we use *Shannon's Capacity Theorem*²⁰ to model the variation of data throughput as a function of SINR as made possible by the range of modulation orders and coding rates available for use in the TDD uplink.

A1.10 Accordingly, if a TDD terminal station radiates continuously at the maximum permitted in-block EIRP of P_{\max} , then it can achieve (subject to zero demand from other TDD terminal stations in the cell) a maximum throughput of

$$C = \xi B \log_2(1 + \text{SINR}_{\text{UL}}) \text{ bits/s}, \quad (1)$$

where B is the noise-equivalent channel bandwidth, SINR_{UL} is the uplink signal-to-interference-plus-noise ratio, and the penalty factor ξ represents the inferiority of the link's spectral efficiency as compared to the Shannon Limit. Furthermore,

$$\text{SINR}_{\text{UL}} = \frac{G P_{\max}}{P_{\text{N}} + P_{\text{I,CC}} + P_{\text{I,AC}}}, \quad (2)$$

where G is the aggregate propagation gain (including receive antenna gain) from the TDD terminal station to the TDD base station, and $P_{\text{N}} = kTB \text{NF}_{\text{BS}}$ is thermal noise power at the TDD base station receiver (k is Boltzman's constant, T is the ambient temperature, and NF_{BS} is the receiver noise figure). $P_{\text{I,CC}}$ and $P_{\text{I,AC}}$ are the co-channel and adjacent-channel interference powers experienced by the TDD base station respectively. The computation of these last two terms is described in later sub-sections of this annex (see Paragraphs A1.33 and A1.43).

A1.11 It should be noted that a TDD terminal station need not radiate at the maximum permitted EIRP in order to achieve maximum throughput in all circumstances. This is because, in practice, radio technologies only support a finite number of modulation and coding schemes, and as such, can not support indefinitely increasing throughputs as a function of increasing SINRs. In other words, there is no utility in achieving a SINR that is greater than an upper threshold, γ_{TH} , as defined by the highest-order modulation and highest-rate coding supported.

A1.12 Therefore, if a TDD terminal station suffers from low levels of path-loss or shadowing, then we may have $\text{SINR}_{\text{UL}} > \gamma_{\text{TH}}$, in which case, the TDD terminal station's in-block EIRP can be reduced (so that $\text{SINR}_{\text{UL}} = \gamma_{\text{TH}}$) with no loss in the achieved throughput. Consequently, we model a TDD terminal station's in-block EIRP, P , as

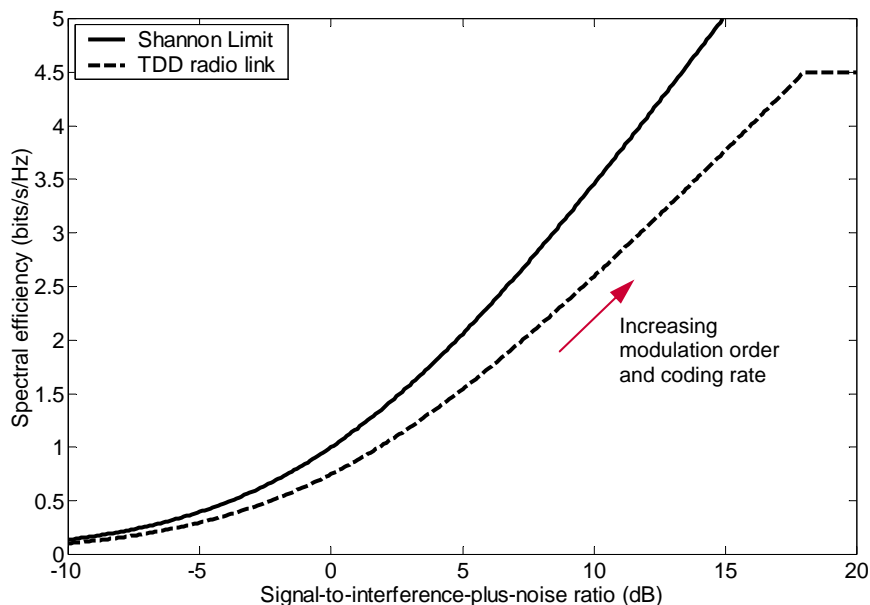
$$P = \begin{cases} P_{\max} & \text{if } \text{SINR}_{\text{UL}} \leq \gamma_{\text{TH}} \\ \frac{\gamma_{\text{TH}}}{\text{SINR}_{\text{UL}}} P_{\max} & \text{if } \text{SINR}_{\text{UL}} > \gamma_{\text{TH}} \end{cases}, \quad (3)$$

²⁰ This describes the upper bound on the spectral efficiency of an additive white Gaussian noise (AWGN) channel. See, for example, *Digital Communications* by J.G.Proakis, 2000, McGraw-Hill.

which in turn means that the resulting uplink SINR and maximum throughput are given by Equation 1 and Equation 2, subject to the constraints that $\text{SINR}_{\text{UL}} \leq \gamma_{\text{TH}}$ and $C \leq \xi B \log_2(1 + \gamma_{\text{TH}})$.

- A1.13 The above formulation implies that a TDD terminal station will always radiate at the minimum power level which would allow it to achieve (via the optimum combination of modulation order and coding rate) the highest uplink throughput possible. It is implicitly assumed that the terminal station transmitter has full knowledge of the uplink channel-state information for the purpose of selecting the most appropriate modulation and coding combination.
- A1.14 Figure 9 shows the variation of C/B with SINR_{UL} used for the purposes of this study. The assumed value of $\xi = 0.75$ is typical of current state of the art in physical layer technologies²¹.
- A1.15 The maximum spectral efficiency of 4.5 bits/s/Hz (via 64-QAM with $\frac{3}{4}$ rate coding, as used in WiMAX) is achieved at a minimum SINR of $\gamma_{\text{TH}} = 18$ dB. In short, a TDD terminal station backs off from radiating at maximum power if the resulting SINR at the TDD base station exceeds $\gamma_{\text{TH}} = 18$ dB.
- A1.16 The throughput in Equation 1 and the EIRP in Equation 3 are used in the next subsection to model the bursty structure of transmissions by individual TDD terminal stations.

Figure 9: Model of spectral efficiency as a function of SINR for the TDD uplink.



b) Bursty transmission and scheduling in the TDD uplink

- A1.17 Modern radio access technologies increasingly employ packet-based transmissions over the air-interface in order to better deal with the bursty nature of traffic, and to more efficiently utilise the radio resource by appropriately scheduling transmissions

²¹ See, for example, *Fundamentals of WiMAX* by J.G.Andrew *et al*, 2007, Prentice-Hall.

to and from those terminal stations associated with favourable radio link conditions at any given instant in time.

A1.18 Consequently, the terminal stations in such systems transmit and receive data in bursts of finite duration. The durations and timing of such bursts are dependent on three factors, namely, a) the throughput that is available to each terminal station, b) the throughput that is required by each terminal station, and c) the manner in which the serving base station schedules communications with each terminal station.

A1.19 In a TDD system, uplink transmissions only occur for a fraction, $u_{UL} < 1$, of the time (i.e., during uplink sub-frames), with the remaining time dedicated to downlink transmissions (i.e., downlink sub-frames). Consequently, the maximum uplink throughput available to a TDD terminal station is equal to $C_{UL} = u_{UL}C$.

A1.20 However, a TDD terminal station may not necessarily require the full uplink throughput available. Indeed, if the terminal station accesses a service which only requires a throughput, R_S , then it only needs to transmit using a fraction,

$$z = \frac{R_S}{C_{UL}} = \frac{R_S}{u_{UL}C} \leq 1, \quad (4)$$

of the time-frequency-code resource available in the uplink.

A1.21 The precise nature of the multiple-access mechanism in an uplink sub-frame is not critically important for the purposes of this study. Nevertheless, it must be noted that if $z > 1$, then the service accessed by the terminal station can not be supported by the TDD network, as this would require more uplink resource than is available within the cell. Moreover, if there are K terminal stations in the cell, requiring fractions, z_i $i = 1 \wedge K$, of the uplink resource, only K' can be supported, where

$$\sum_{i=1}^{K'} z_i \leq 1. \quad (5)$$

A1.22 The identities of the K' supported TDD terminal stations are decided by the TDD base station through a process of scheduling.

A1.23 Many different scheduling algorithms exist. If fairness is the objective, the base station may schedule terminals in a round-robin fashion. If the objective is to maximize the uplink throughput, the base station may, at any given time, schedule the terminal(s) with the highest uplink SINR. If the objective is to maximize the number of satisfied customers, the base station may schedule terminals in order of ascending z_i .

A1.24 For the purposes of this study, we are interested in the scheduling of TDD terminal stations only in so far as it impacts the levels of interference generated towards FDD terminal stations. For this reason, we use the latter scheduling algorithm described above in order to allow the largest number of TDD terminal stations to radiate during each scheduling interval.

A1.25 To further clarify the scheduling model adopted, we present below an example based on the timing parameters of the WiMAX physical layer.

Example

- 1.25.1 Consider a scheduling interval of $T = 20$ ms containing $N_F = 4$ WiMAX frames of $T_F = 5$ ms duration each. Our assumption is that, in order to maintain real-time communication, a terminal station must be serviced (at an appropriate throughput) once every 20 ms. We have selected 20 ms, as this is the time epoch associated with the encoding interval of many audio and video compression technologies.
- 1.25.2 If $u_{UL/DL}$ is the ratio of time reserved for uplink over that reserved for downlink, then

$$u_{UL} = \frac{u_{UL/DL}}{1 + u_{UL/DL}}. \quad (6)$$

- 1.25.3 A value of $u_{UL/DL} = 1/3$ is commonly quoted for WiMAX, in which case $u_{UL} = 1/4$. This means that each of the four 5 ms WiMAX frames in the 20 ms scheduling interval is divided into a downlink sub-frame of $T_{DL} = 3.75$ ms and an uplink sub-frame of $T_{UL} = 1.25$ ms. This is illustrated in Figure 10.
- 1.25.4 We next consider $K' = 5$ terminal stations requiring fractions $z_1 = 0.1$, $z_2 = 0.1$, $z_3 = 0.2$, $z_4 = 0.2$, and $z_5 = 0.3$, respectively of the available uplink resource over the scheduling interval.
- 1.25.5 Figure 10 shows the scheduling of the terminal stations in ascending order of required resources, z_i , over a scheduling interval of 20 ms. To appreciate the impact of scheduling on the nature of the TDD terminal stations as sources of interference, we focus on the case of the 3rd terminal station.
- 1.25.6 If the fraction, z_3 , of the uplink radio resource required by this terminal station was equal to 0.25, and took up all the time-frequency-code resource within an otherwise unoccupied uplink sub-frame, one could conclude that the terminal station would radiate at an in-block EIRP level of P (as derived in Equation 3) over the relevant uplink sub-frame.
- 1.25.7 However, in the presented example, the fraction, z_3 , of the uplink radio resource required by the 3rd terminal station is equal to 0.2, and is split into $z_{3,1} = 0.05$ and $z_{3,2} = 0.15$ between the 1st and 2nd uplink sub-frames respectively. One may then conclude that the 3rd terminal station effectively appears as an interferer which radiates at in-block EIRP levels of $(0.05/0.25)P$ and $(0.15/0.25)P$ when averaged over each of the 1st and 2nd uplink sub-frames respectively.
- A1.26 Expressing the previous example in general terms, we can see that when scheduling is performed over N_F uplink sub-frames, the k^{th} TDD terminal effectively *appears* as an interferer which radiates at an in-block EIRP level of

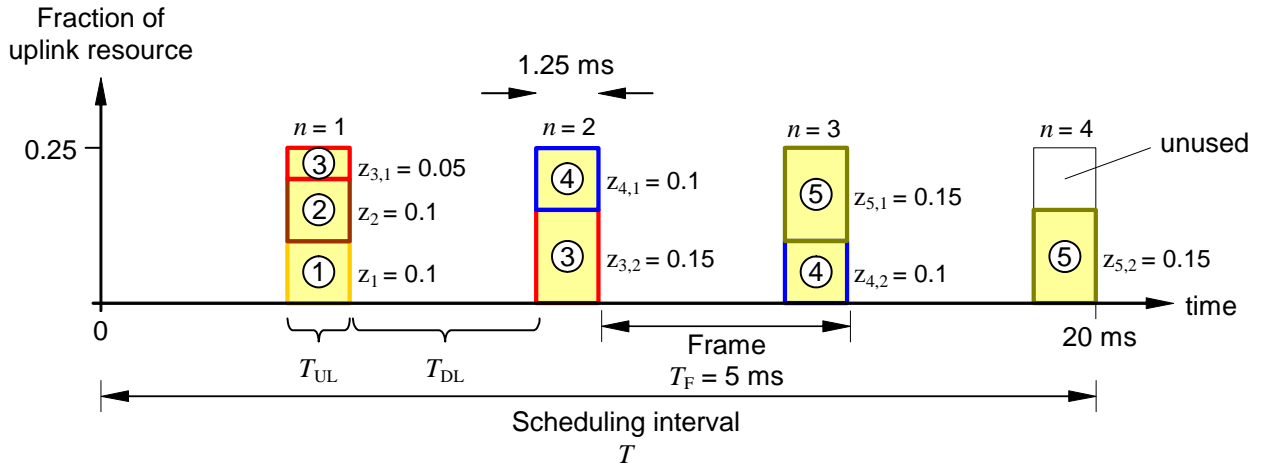
$$P_{k,n} = \alpha_{k,n} P_k \quad (7)$$

when averaged over the n^{th} uplink sub-frame, where

$$\alpha_{k,n} = \frac{z_{k,n}}{(1/N_F)}, \quad (8)$$

$z_{k,n}$ is the fraction of the uplink resource that is available in the n^{th} uplink sub-frame and which is required by the k^{th} terminal station, and P_k is the actual in-block EIRP level of the k^{th} terminal station as derived in Equation 3.

Figure 10: Example of uplink scheduling by a TDD base station of five terminal stations requiring fractions {0.1, 0.1, 0.2, 0.2, 0.3} of the uplink radio resource.



A1.27 The effective in-block EIRP values, $P_{k,n}$, derived in Equation 7 will be used in Equation 15 later in this annex to compute the adjacent-channel interference from TDD terminal stations to FDD terminal stations.

c) Co-channel interference in the TDD uplink

A1.28 Co-channel interference at a TDD base station can, in principle, originate from both TDD base stations and TDD terminal stations.

A1.29 In practice, however, it is highly likely that the uplink/downlink phases across the co-channel cells of a TDD network will be synchronised in order to avoid base-to-base and (particularly) terminal-to-terminal interference. In such a case, co-channel interference at a TDD base station would only originate from radiations of TDD terminal stations realised in the form of intra-cell and inter-cell interference. This has been assumed in our analysis.

Intra-cell (multiple-access) interference

A1.30 In technologies such as WiMAX, the combined use of OFDMA and/or TDMA on the uplink implies a nominal absence of intra-cell (or multiple-access) interference. For this reason, we do not model intra-cell co-channel interference in our analysis, and assume this to be zero.

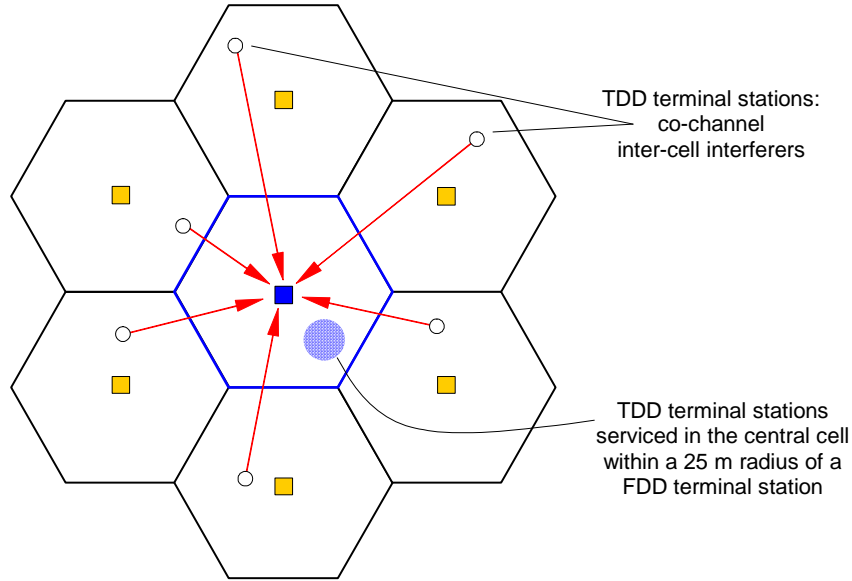
Inter-cell interference

A1.31 A precise modelling of co-channel inter-cell interference on the uplink is complicated, as this requires the detailed characterisation of a large number of terminal stations in the adjacent cells, whose behaviour in turn depends on the

interference environment in those cells. Simplified models are therefore often adopted.

A1.32 For the purposes of this study, we model the co-channel inter-cell interference experienced at a TDD base station as the sum of received signals originating from single TDD terminal stations located randomly in each adjacent cell, radiating at the maximum permitted in-block EIRP, P_{\max} , and occupying all the radio resource available in every uplink sub-frame. This is illustrated in Figure 11 below.

Figure 11: Model for co-channel inter-cell interference in the TDD uplink.



A1.33 The co-channel interference experienced by the central-cell TDD base station from radiations in M adjacent cells may then be written as

$$P_{\text{I,CC}} = P_{\max} \sum_{i=1}^M G_i, \quad (9)$$

where G_i is the aggregate path-gain (including receive antenna gain) from the TDD terminal station in the i^{th} adjacent cell to the TDD base station in the central cell, and P_{\max} is the maximum permitted terminal station in-block EIRP.

A1.34 The uplink SINR at the central-cell base station can then be computed by substituting Equation 9 into Equation 2.

A1.35 In practice, there will be instances when the TDD terminal stations in the adjacent cells do not radiate at the maximum permitted in-block EIRP (e.g., due to their proximity to the serving base station or low levels of shadowing). In such instances, the model of Equation 9 would overestimate the amount of co-channel inter-cell interference experienced at the TDD base station.

A1.36 On the other hand, there will be instances where more than a single TDD terminal radiates in each of the adjacent cells, and some of these may be located closer to the central cell than the single TDD terminal station we have considered. In such

instances, the model of Equation 9 would underestimate the amount of co-channel inter-cell interference experienced at the TDD base station.

- A1.37 Despite its limitations, the adopted model provides a reasonably accurate representation of the co-channel inter-cell interference experienced at a TDD base station.
- A1.38 In deriving the results presented in Section 4 of this document, we have assumed the model of Equation 9 with a ring of $M = 6$ adjacent cells. Furthermore, P_{\max} is set to 31 and 25 dBm/(5 MHz) for the modelling of TDD macro-cells and pico-cells respectively.

d) Adjacent-channel interference in the TDD uplink

- A1.39 Adjacent-channel interference at a TDD base station can, in principle, originate from the radiations of FDD or TDD terminal stations and base stations in adjacent frequency blocks.
- A1.40 Adjacent-channel interference from TDD terminal stations to TDD base stations is typically not a significant source of degradation in the uplink SINR (the exception being rare geometries where the interfering terminal station is extremely close to the victim base station). Also note that the TDD base stations of interest in this study operate in frequency blocks that are adjacent to the FDD downlink spectrum. Consequently, adjacent-channel interference from FDD terminal stations is not an issue.
- A1.41 Moreover, it is highly likely that the uplink/downlink phases of TDD radio links in neighbouring frequency blocks will be synchronised, particularly if they are managed by the same operator. Consequently, adjacent-channel interference from TDD base stations to TDD base stations is also unlikely in the frequency blocks of interest.
- A1.42 The only remaining source of adjacent-channel interference at the TDD base stations of interest is due to radiations by FDD base stations. As explained in Ofcom's Statement¹⁷ of April 2008, such interference can be effectively mitigated via adequate spatial separation between the base stations (100 m for a 1 dB desensitisation).
- A1.43 Given the above arguments, and for the purposes of this study, we make the simplifying assumption that the TDD uplink does not suffer from significant adjacent-channel interference, i.e., that $P_{I,AC} = 0$ in Equation 2.

Modelling of the FDD downlink

- A1.44 In this sub-section, we describe in detail the methodology employed for calculating the FDD downlink throughput, and for the modelling of collisions between TDD uplink packets and FDD downlink packets.

a) Adaptive modulation and coding in the FDD downlink

- A1.45 Following the same principles adopted for the TDD uplink, we use *Shannon's Capacity Theorem* to model the variation of data throughput as a function of SINR as made possible by the range of modulation orders and coding rates available for use in the FDD downlink. It is implicitly assumed that the base station transmitter

has full knowledge of the downlink channel-state information for the purpose of selecting the most appropriate modulation and coding combination.

- A1.46 Accordingly, if a FDD base station radiates continuously at the maximum permitted in-block EIRP of P_{\max} , then it can potentially achieve a maximum downlink throughput of

$$C = \xi B \log_2(1 + \text{SINR}_{\text{DL}}) \text{ bits/s}, \quad (10)$$

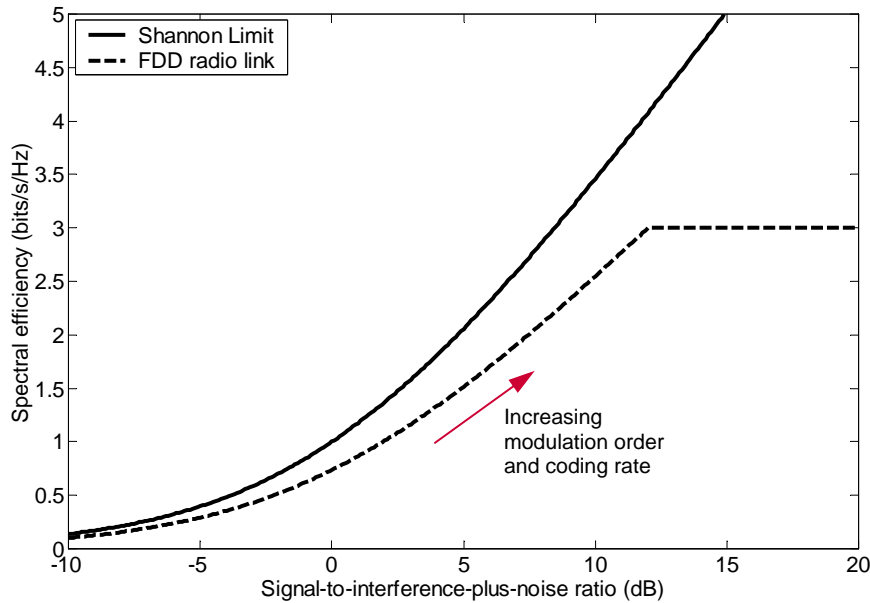
where B is the noise-equivalent channel bandwidth, SINR_{DL} is the downlink signal-to-interference-plus-noise ratio, and the penalty factor ξ represents the inferiority of the link's spectral efficiency as compared to the Shannon Limit. Furthermore,

$$\text{SINR}_{\text{DL}} = \frac{G P_{\max}}{P_{\text{N}} + P_{\text{I,CC}} + P_{\text{I,AC}} + P_{\text{I,IM}}}, \quad (11)$$

where G is the aggregate propagation gain (including receive antenna gain) from the FDD base station to the FDD terminal station, and $P_{\text{N}} = kTB \text{NF}_{\text{TS}}$ is thermal noise power at the FDD terminal station receiver (k is Boltzman's constant, T is the ambient temperature, and NF_{TS} is the receiver noise figure). $P_{\text{I,CC}}$, $P_{\text{I,AC}}$, and $P_{\text{I,IM}}$ are the co-channel, adjacent-channel, and inter-modulation interference powers experienced by the FDD terminal station respectively. The computation of these last three terms is described in later sub-sections of this annex (see Paragraphs A1.56, A1.69, and A1.78).

- A1.47 Figure 12 shows the variation of C/B with SINR_{DL} used for the purposes of this study. The assumed value of $\xi = 0.75$ is typical of current state of the art in physical layer technologies. The maximum spectral efficiency of 3 bits/s/Hz (via 16-QAM with $\frac{3}{4}$ rate coding, as used in UTRA-FDD HSDPA) is achieved at a minimum SINR of $\gamma_{\text{TH}} = 12$ dB.

Figure 12: Model of spectral efficiency as a function of SINR for the FDD downlink.



- A1.48 We assume that a FDD base station will always radiate at the minimum power level which would allow it to achieve (via the optimum combination of modulation order and coding rate) the highest downlink throughput possible. This means that a FDD base station backs off from radiating at full power if the resulting SINR at the FDD terminal station exceeds $\gamma_{\text{TH}} = 12$ dB (see Figure 12). In short, the resulting downlink SINR and maximum throughput are given by Equation 10 and Equation 11, subject to the constraints that $\text{SINR}_{\text{DL}} \leq \gamma_{\text{TH}}$ and that $C \leq \xi B \log_2(1 + \gamma_{\text{TH}})$.
- A1.49 What is of particular interest in this study is the downlink throughput achieved by the reception at a FDD terminal station of a downlink radio packet of duration T_P over a scheduling interval T . The FDD downlink throughput averaged over the scheduling interval is then given by

$$C_{\text{DL}} = \frac{T_P}{T} C. \quad (12)$$

- A1.50 The cumulative probability distributions of FDD downlink throughput presented in Section 4 of this document correspond to the statistics of C_{DL} in Equation 12 for $T_P = 2$ ms and $T = 20$ ms. Specifically, the statistics of C_{DL} are first computed with $P_{\text{I,AC}}$ and $P_{\text{I,IM}}$ set to zero in Equation 11, representing the absence of TDD terminal station interferers. The impairments in FDD downlink throughput as a result of radiations by TDD terminal stations are then evaluated by including the computed values of $P_{\text{I,AC}}$ and $P_{\text{I,IM}}$ in the denominator of Equation 11.
- A1.51 We next describe the computation of parameters $P_{\text{I,CC}}$, $P_{\text{I,AC}}$ and $P_{\text{I,IM}}$.

b) Co-channel interference in the FDD downlink

- A1.52 Co-channel interference at a FDD terminal station originates from FDD base station radiations in the form of intra-cell and inter-cell interference.

Intra-cell (multiple-access) interference

- A1.53 In this study, we evaluate the maximum downlink throughput potentially available to a FDD terminal station due to the reception of a downlink radio packet. For this reason, we do not model any intra-cell (multiple-access) co-channel interference, and assume this to be zero.

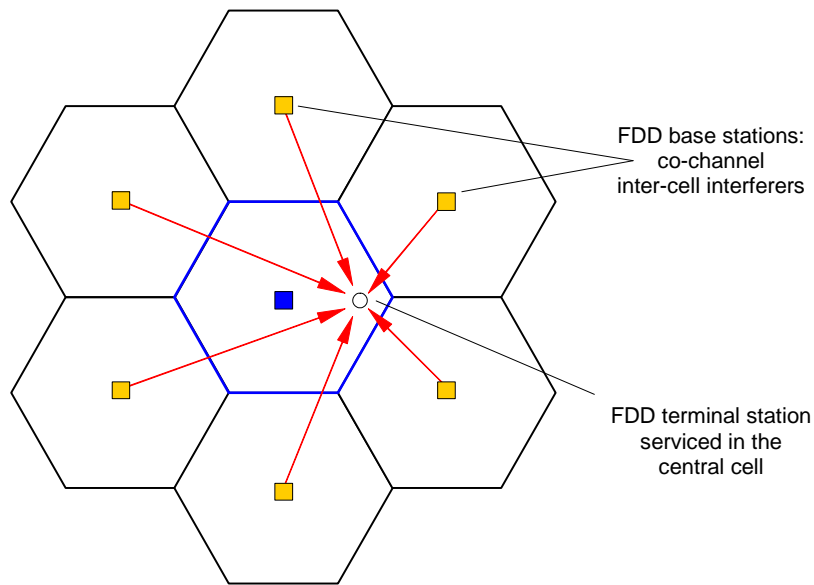
Inter-cell interference

- A1.54 The inter-cell co-channel interference experienced by a FDD terminal station is caused by co-channel radiations from FDD base stations in adjacent cells. This may be written in a general form as

$$\sum_{m=1}^M G_m \eta_m P_m, \quad (13)$$

where M is the number of adjacent-cell FDD base stations, G_m is the total path-gain (including receive antenna gain) from the m^{th} FDD base station to the receiving FDD terminal station, and P_m is the in-block EIRP of the m^{th} FDD base station. The interference scenario is illustrated in Figure 13. The significance of the multiplier η_m is described next.

Figure 13: Model for co-channel inter-cell interference in the FDD downlink.



A1.55 To precisely model the inter-cell interference in a system such as UTRA-FDD HSDPA, one needs to account for the loading and traffic conditions in each adjacent cell. These influence a) the power radiated by each interfering base station, and b) the probability of collision between downlink radio packets in adjacent asynchronous cells.

A1.56 At a coarse level, these effects may be expressed via the multiplier η_m . For the purposes of this study, we assume that all adjacent cells are fully loaded, to the extent that the corresponding FDD base stations radiate continuously and at the maximum permitted in-block EIRP, P_{\max} , so that $\eta_m = 1$ and $P_m = P_{\max}$ for $m = 1 \wedge M$. As a result, Equation 13 may be re-written as

$$P_{I,CC} = P_{\max} \sum_{m=1}^M G_m \cdot \quad (14)$$

A1.57 The SINR at the FDD terminal station receiver (and hence the FDD downlink throughput) can then be computed by substituting Equation 14 into Equation 11.

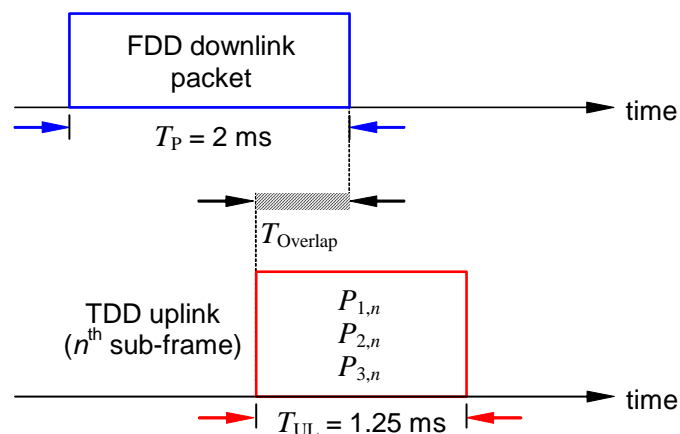
A1.58 In practice, the FDD base stations in adjacent cells do not always transmit data continuously, and in instances where they might transmit continuously, they would not necessarily do so at the maximum permitted EIRP (e.g., due to the proximity of the serviced terminal stations). Therefore, the model of Equation 14 defines an upper bound on the co-channel inter-cell interference experienced at a FDD terminal station.

A1.59 In deriving the results presented in Section 4 of this document, we have assumed the model of Equation 14 for a ring of $M = 6$ adjacent cells with P_{\max} set to 61 dBm/(5 MHz).

c) Adjacent-channel interference in the FDD downlink

- A1.60 Adjacent-channel interference at a FDD terminal station can, in principle, originate from the radiations of TDD terminal stations and FDD or TDD base stations in adjacent frequency blocks.
- A1.61 Adjacent-channel interference from FDD base stations to FDD terminal stations is typically not a significant source of degradation in the downlink SINR (the exception being rare geometries where the victim terminal station is extremely close to the interfering base station). Furthermore, this type of interference is characteristic of all FDD cellular deployments and is in no way unique to the 2.6 GHz band. Moreover, adjacent-channel interference from TDD base stations is no greater (and, due to bursty transmissions, is typically lower) than that from FDD base stations.
- A1.62 For the above reasons, we do not model the adjacent-channel interference from base stations in our study of the FDD downlink throughput.
- A1.63 We instead focus on the far more significant adjacent-channel interference from TDD terminal stations (whose characteristics were described earlier in this annex).
- A1.64 Radiations by TDD terminal stations only cause interference towards a FDD terminal station if a received FDD downlink packet overlaps in time (i.e., collides) with the radiated TDD uplink packets. The extent of this interference is a function of the degree of overlap, the identities (and hence the proximities) of the TDD terminal stations involved, and their effective radiation powers in the relevant uplink sub-frames. To clarify the above issues, we present our model using the example below.
- A1.65 Figure 14 illustrates a scenario where a FDD downlink packet of duration $T_p = 2$ ms (as in UTRA-FDD HSDPA) partially collides with the n^{th} TDD uplink sub-frame of duration $T_{UL} = 1.25$ ms (as in WiMAX) containing transmissions from $K = 3$ TDD terminal stations. The *effective* in-block EIRPs of these terminal stations are $P_{k,n}$ for $k = 1, 2, 3$, where $P_{k,n} = \alpha_{k,n} P_k$ (see Equation 7).

Figure 14: Example of collision between a FDD downlink packet and TDD packets in the n^{th} uplink sub-frame.



A1.66 It is clear from Figure 14 that, when *averaged*²² over the FDD downlink packet interval, the effective in-block EIRP of the k^{th} TDD terminal station is given by

$$\frac{T_{\text{Overlap}}}{T_{\text{P}}} P_{k,n} = \frac{T_{\text{Overlap}}}{T_{\text{P}}} \alpha_{k,n} P_k, \quad (15)$$

where T_{Overlap} is the overlap interval, and P_k is the actual in-block EIRP level of the k^{th} terminal station as derived in Equation 3.

A1.67 We assume that the arrival time of the FDD downlink packet within the scheduling interval, T , follows a uniform random distribution. As such, the FDD downlink packet may collide with any one of $N_{\text{F}} = 4$ TDD uplink sub-frames over a 20 ms scheduling interval.

A1.68 The total power of the adjacent-channel interferers received at the antenna connector of the FDD terminal station is then given by

$$P_{\text{AC}} = \frac{T_{\text{Overlap}}}{T_{\text{P}}} \sum_{k=1}^K G_k \alpha_{k,n} P_k. \quad (16)$$

where K is the total number of TDD terminals stations radiating in the proximity (e.g., within a 25 m radius) of the receiving FDD terminal station, and G_k is the aggregate path-gain (including receive antenna gain) from the k^{th} TDD terminal station to the receiving FDD terminal station.

A1.69 Note that P_{AC} is the total received interferer power generated by the TDD terminal stations radiating in different adjacent frequency blocks respectively (synchronised uplink/downlink phases are assumed across the TDD blocks). The adjacent-channel interference experienced by the FDD terminal station may then be written as

$$P_{\text{I,AC}} = \frac{T_{\text{Overlap}}}{T_{\text{P}}} \sum_{k=1}^K \frac{G_k \alpha_{k,n}}{A_k} P_k, \quad (17)$$

where A_k is the adjacent-channel interference ratio (ACIR)²³ associated with the radio link from the k^{th} TDD terminal station to the FDD terminal station. This accounts for interferer radiation masks and non-ideal receiver frequency discrimination.

A1.70 The SINR at the FDD terminal station receiver (and hence the FDD downlink throughput) can then be computed by substituting Equation 17 into Equation 11.

A1.71 The modelling of saturation and inter-modulation effects are described next.

²² This is a coarse model which does not take into account of the precise nature of the multiple-access mechanism within the TDD uplink sub-frame.

²³ The ACIR is defined as the ratio of the power of an adjacent-channel interferer as received at the victim, divided by the interference power experienced by the victim receiver as a result of both transmitter and receiver imperfections.

Saturation

- A1.72 The components in the receiver chain of a FDD terminal station are unable to deal with arbitrarily large signal levels. If the absolute values of the received adjacent-channel signals are beyond a certain threshold the receiver will be overloaded or saturated. The performance of the receiver is difficult to model in such circumstances. In our model we assume that the saturation of the receiver would result in a zero radio link throughput.
- A1.73 As illustrated in Figure 2 of Section 4, the FDD terminal station's receiver is to some extent protected from certain adjacent-channel interferers by its front-end (duplex) filter. The extent of this protection depends on whether the adjacent-channel interferers fall within the pass-band, transition-band, or stop-band of the front-end filter. Based on this formulation, the FDD downlink throughput is assumed to fall to zero if

$$P_X = \frac{T_{\text{Overlap}}}{T_P} \sum_{k=1}^K G_k G_{X,k} \alpha_{k,n} P_k > \Pi_{\text{Sat}}, \quad (18)$$

where $G_{X,k} \leq 1$ is the gain of the FDD terminal station's front-end filter at the frequency of the k^{th} TDD terminal station interferer, Π_{Sat} is the adjacent-channel power threshold beyond which the FDD terminal station can be assumed to be saturated, and P_X is the total adjacent-channel interferer power at the output of the front-end filter.

- A1.74 Measurements commissioned by Ofcom of commercially available UTRA-FDD user equipment in the 2.1 GHz band suggest that Π_{Sat} is approximately -10 dBm in practice. This value is used in our modelling of saturation effects.
- A1.75 We account for the roll-off of the front-end filter via gains, $G_{X,k}$, of 0, -4 , -8 , and -12 dB for interferers in frequency blocks #24, #23, #22, and #21 respectively. Interferers in frequency blocks #35, #36, #37, and #38 fall within the pass-band of the front-end filter (which nominally spans from 2620 to 2690 MHz) and $G_{X,k} = 0$ dB for interferers in these frequency blocks.

Inter-modulation

- A1.76 Let $P_{\text{I,IM}}$ be the interference power experienced by the FDD terminal station receiver as a result of co-channel third-order inter-modulation products generated by adjacent-channel interferers received at aggregate powers of P_{AC1} and P_{AC2} , and at frequency offsets Δf and $2\Delta f$ from the wanted signal carrier. It can be shown that

$$P_{\text{I,IM}} = \lambda P_{\text{AC1}}^2 P_{\text{AC2}}, \quad (19)$$

where λ is a constant of proportionality.

- A1.77 Let us also assume that the third-order inter-modulation products generated by equal-power adjacent-channel interferers, each received at power Π_{AC} , and at frequency offsets Δf and $2\Delta f$ respectively from the wanted signal carrier, result in a 3 dB desensitisation of the receiver with respect to the receiver's reference

sensitivity performance²⁴. By definition, the 3 dB desensitisation implies that the inter-modulation interference power experienced by the receiver is equal to the thermal noise power, P_N ; i.e., that,

$$P_N = \lambda \Pi_{AC}^2 \Pi_{AC} \quad (20)$$

where $P_N = k T B \text{NF}_{TS}$, k is Boltzmann's constant, T is the ambient temperature, B is the receiver's noise-equivalent bandwidth, and NF_{TS} is the receiver's noise figure.

A1.78 Dividing Equation 19 by Equation 20, we have

$$P_{I,IM} = \left(\frac{P_{AC1}}{\Pi_{AC}} \right)^2 \left(\frac{P_{AC2}}{\Pi_{AC}} \right) P_N. \quad (21)$$

A1.79 In summary, Equation 21 describes the experienced inter-modulation interference, $P_{I,IM}$, as a function of the aggregate adjacent-channel interferer powers, P_{AC1} and P_{AC2} , given the reference adjacent-channel power, Π_{AC} , and the thermal noise power P_N .

A1.80 Note that the adjacent-channel interferer aggregate powers, P_{AC1} and P_{AC2} are computed by application of Equation 18 in each of the relevant frequency channels respectively²⁵.

A1.81 The interference power, $P_{I,IM}$, is substituted into the denominator of Equation 11 in order to compute the downlink SINR at the FDD terminal station. In scenarios where interferers in more than two adjacent channels are involved (e.g., see Figure 2), we apply Equation 21 to every pair of channel offsets which can give rise to inter-modulation products that are co-channel with the wanted signal, and then add the results prior to substitution into the denominator of Equation 11.

A1.82 The reference power, Π_{AC} , of the adjacent-channel interferers can be derived either from the relevant minimum requirement specifications in technical standards, or via direct measurement of FDD terminal station receivers.

A1.83 For example, 3GPP TS 25.101 specifies that the inter-modulation characteristics of a FDD terminal station receiver should be such that the reception of two interferers, each at a level of -46 dBm and at frequency offsets of 10 and 20 MHz from the wanted carrier, should at most result in a 3 dB desensitisation with respect to the reference sensitivity performance; i.e., $\Pi_{AC} = -46$ dBm.

A1.84 Measurements commissioned by Ofcom of commercially available UTRA-FDD user equipment in the 2.1 GHz band suggest that Π_{AC} is closer to -30 dBm in practice. This value is used in our modelling of inter-modulation effects.

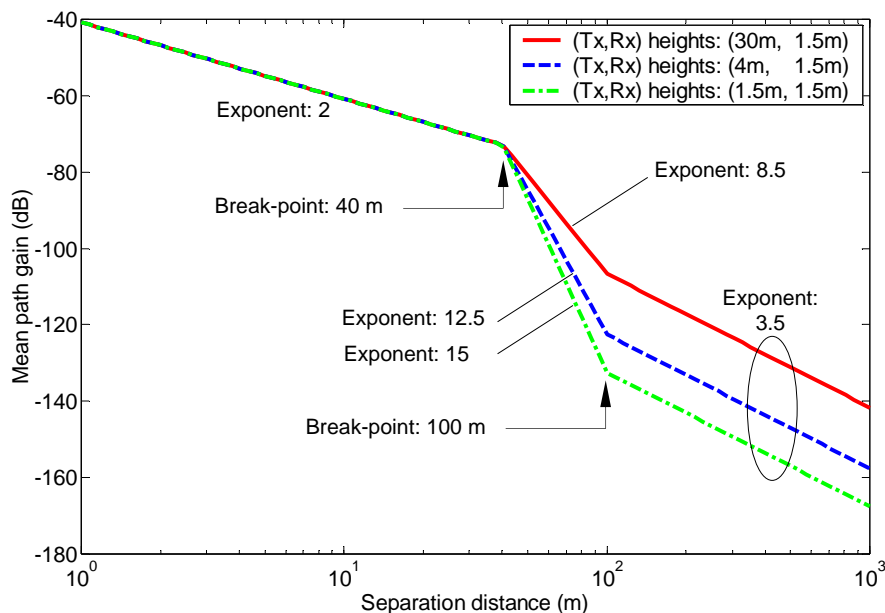
²⁴ Reference sensitivity performance refers to the case where the only source of degradation in the receiver is additive thermal noise.

²⁵ The interferer powers P_{AC1} and P_{AC2} are usually cited as measured at the antenna connector, and as such, strictly speaking, should be calculated via Equation 16. However, the front-end filter gains in Equation 18 account for the fact that interferers in frequency blocks #21 to #24 are attenuated prior to their processing by the active elements of the FDD terminal station receiver.

Propagation models

- A1.85 Path-loss exponents similar to those implied by the extended (urban) Hata model²⁶ are used to characterise mean path-loss over all radio links, assuming antenna heights (above ground level) of 30 and 1.5 metres for base stations and terminal stations respectively.
- A1.86 For pico-cell base stations, a reduced antenna height of 4 metres above ground level was also considered, although the results presented in Section 4 were insensitive to this height reduction.
- A1.87 The corresponding variations of mean path-loss as a function of separation are illustrated in Figure 15 for different transmit-receive antenna height combinations at a frequency of 2.6 GHz. The mean path-loss is modelled as free-space propagation (exponent of 2) for all distances less than 40 metres.

Figure 15: Mean path-loss for different transmit-receive antenna height combinations.



- A1.88 For all base-terminal links, shadowing standard deviations of 3.5 dB and 12 dB are assumed for separations of less than 40 metres and greater than 40 metres respectively. Minimum base-terminal separation of 50 and 5 metres are also assumed in macro-cells and pico-cells respectively.
- A1.89 For terminal-to-terminal links, a shadowing standard deviation of 3.5 dB is assumed for all separations²⁷.

²⁶ European Radiocommunications Office, "SEAMCAT user manual (Software version 2.1)," February 2004.

²⁷ This is broadly in line with the values specified in "Tn Channel Models (IEEE 802.11-03/940r2)," High Throughput Task Group, IEEE P802.11, 15 March 2004.

Summary of parameter values

A1.90 Here we present a list of all parameter values assumed in the derivation of the results of Section 4 and as described in this annex. BS and TS denote base station and terminal station respectively.

Table 3: List of FDD parameter values.

FDD

BS maximum in-block EIRP, P_{\max}	61 dBm (Tx power: 44 dBm)
TS antenna gain	0 dBi
Noise-equivalent channel bandwidth, B	3.84 MHz
TS noise figure, NF_{TS}	9 dB
Maximum DL SINR via power control and AMC, γ_{TH}	12 dB
Cell radius	1000 metres
BS antenna height	30 metres
Minimum BS-TS separation	50 metres
Downlink packet duration, T_p	2 ms
TS front-end filter gain, $G_{X,k}$	0, -4, -8, -12 dB @ blocks #24, #23, #22, #21 0 dB @ blocks #35, #36, #37, #38
TS third-order inter-modulation reference interferer power, Π_{AC}	-30 dBm
TS saturation threshold, Π_{Sat}	-10 dBm

Table 4: List of TDD parameter values.

TDD

TS maximum in-block EIRP, P_{\max}	31 dBm (macro-cell) 25 dBm (pico-cell)
BS antenna gain	17 dBi (macro-cell) 3 dBi (pico-cell)
Noise-equivalent channel bandwidth, B	4.1 MHz
BS noise figure, NF_{BS}	5 dB
Maximum SINR achieved by power control and AMC, γ_{TH}	18 dB
Cell radius	1000 metres (macro-cell) 100 metres (pico-cell)
BS antenna height	30 metres (macro-cell) 4 metres (pico-cell)
TS spatial density per 5 MHz block	$1/10/2/2/18 \text{ metre}^{-2}$
Minimum BS-TS separation	50 metres (macro-cell) 5 metres (pico-cell)
Uplink/downlink ratio, $u_{\text{UL/DL}}$	1:3
Frame duration, T_F	5 ms

Table 5: List of generic parameter values.

General

Operating frequency	2.6 GHz
Number of Monte-Carlo trials	5000
TS-TS separation	25 metres (max) 1 metre (min)
TS-TS link adjacent-channel interference ratio (ACIR)	(33, 45, 53, 61) dB (TDD macro-cell) (40, 50, 61, 64) dB (TDD pico-cell) @ the (1 st , 2 nd , 3 rd , 4 th) adjacent channels
Service Rate, R_S	30 kbits/s over scheduling interval (VOIP)
Scheduling interval, T	20 ms
Boltzmann's constant, k	1.3804×10^{-23}
Ambient temperature, T	290 Kelvin

Annex 2

Terminal station transmission characteristics

Introduction

- A2.1 In this annex we quantify the potential for spectral leakage into adjacent (5 MHz) blocks as a result of radiations by terminal stations within the 2.6 GHz band.
- A2.2 We first compute the adjacent-channel leakage ratios (ACLRs) that are required in order for a terminal station to comply with the limits at the corner frequencies of the relevant SE42 block-edge mask (BEM), when the terminal station radiates at the maximum permitted in-block EIRP. The derived ACLR values are used in the analysis presented in Section 4 of this document to characterise terminal stations which are served by TDD macro-cells.
- A2.3 We subsequently present commissioned measurements²⁸ of commercially available UTRA-FDD user equipment (UE) operating in the 2.1 GHz band. We use the measurement results as a means of identifying realistic levels of spectral leakage caused by the type of terminal station equipment which might be deployed in the 2.6 GHz band, when radiating at less than the maximum permitted in-block EIRP. The ACLR values derived are used in the analysis presented in Section 4 of this document to characterise terminal stations which are served by TDD pico-cells.

Spectral leakage with terminal stations operating at the maximum permitted EIRP

- A2.4 The technical conditions adopted by Ofcom in relation to the use of the 2.6 GHz band by terminal stations are in line with those developed by the SE42 project team²⁹, and are summarised below:
- A terminal station in-block mean total radiated power (TRP)³⁰ of 31 dBm/(5 MHz) will apply for all frequency blocks.
 - All terminal station types will be subject to a single block-edge mask (BEM) profile. This BEM is broadly similar to the 3GPP TS 25.101 user equipment spectrum emission mask minimum (relative) requirements based on a transmission power of 30 dBm/(3.84 MHz).

²⁸ ERA Technology, "Measurements of UTRA-FDD user equipment characteristics in the 2.1 GHz band," final report, April 2008. Document is available at: <http://www.ofcom.org.uk/consult/condocs/2ghzregsnotice/>.

²⁹ "Report from CEPT to the European Commission in response to the Mandate to develop least restrictive technical conditions for frequency bands addressed in the context of WAPECS," CEPT Report 19, December 2007.

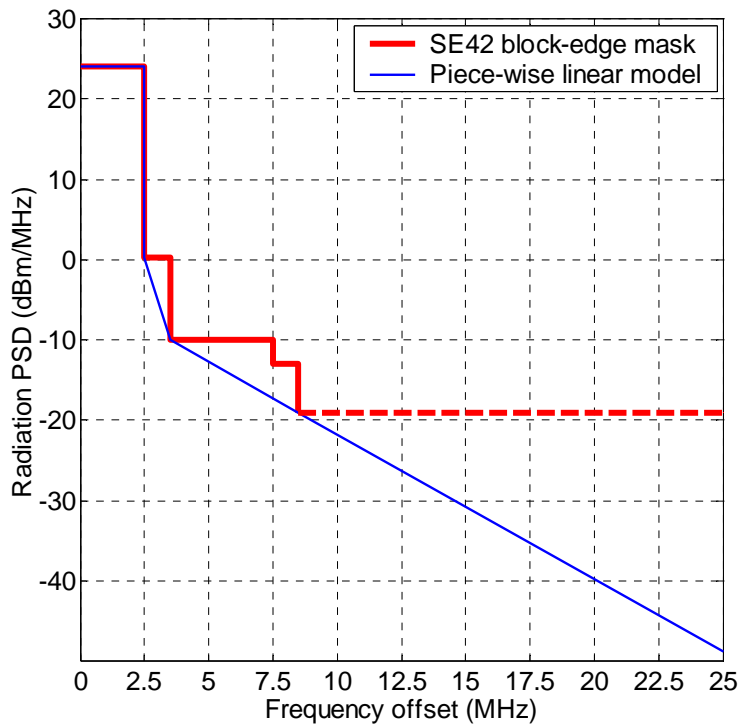
³⁰ For omni-directional transmissions, the specified TRP is equivalent to a mean EIRP of 31 dBm/(5 MHz), but allows the possibility of increased EIRP in specific directions subject to appropriate reductions of EIRP in other directions.

A2.5 The adopted terminal station BEM is detailed in Table 6 below, and is illustrated in Figure 16 (thick line) in conjunction with the maximum permitted in-block mean EIRP of 31 dBm/(5 MHz). For clarity, all power levels are normalised to units of dBm/MHz.

Table 6: SE42 BEM for terminal stations.

Frequency	Maximum mean EIRP for out-of-block emissions
From 2470 MHz to offset of –6 MHz from lower block edge	–19 dBm/MHz
Offsets of –6.0 to –5.0 MHz from lower block edge	–13 dBm/MHz
Offsets of –5.0 to –1.0 MHz lower block edge	–10 dBm/MHz
Offsets of –1.0 to 0.0 MHz lower block edge	–15 dBm/30kHz
Offsets of 0.0 to +1.0 MHz upper block edge	–15 dBm/30MHz
Offsets of +1.0 to +5.0 MHz upper block edge	–10 dBm/MHz
Offsets of +5.0 to +6.0 MHz upper block edge	–13 dBm/MHz
Offset of +6.0 MHz from upper block edge to 2720 MHz	–19 dBm/MHz

Figure 16: SE42 BEM for terminal stations, along with a piece-wise linear model for a terminal station’s radiation power spectral density, as a function of frequency offset from the carrier.



A2.6 As can be seen, the SE42 BEM is characterised by sharp step-changes at a number of so-called “corner” frequencies, as well as by a constant emission limit (i.e., zero roll-off) for frequency offsets greater than 6 MHz from the block edge.

- A2.7 In practice, the radiation power spectral density (PSD) of a terminal station is different from the SE42 BEM in two key respects: a) the radiation PSD is a continuous (i.e., smooth) function of frequency; and b) the radiation PSD tends to decrease broadly monotonically – at least over the first few adjacent channels – as a function of frequency offset from the carrier (notwithstanding inter-modulation components and spurious emissions). Nevertheless, in order to achieve compliance with the regulatory requirements, the radiation PSD of a terminal station must be upper-bounded by the SE42 BEM.
- A2.8 Given the above observations, the radiation PSD of a terminal station which operates at the maximum permitted in-block EIRP may be modelled by a simple piece-wise linear profile which lies just below the SE42 BEM at the critical corner frequencies, and is associated with a constant roll-off gradient of $-9/5$ dB/MHz for frequency offsets greater than 1 MHz from the block edge. Such a PSD profile is illustrated in Figure 16 (thin line).
- A2.9 The ACLR of a signal is defined as the ratio of the signal's power (nominally equal to the power over the signal's pass-band) divided by the power of the signal when measured at the output of a (nominally rectangular) receiver filter centred on an adjacent frequency channel.
- A2.10 Accordingly, numerical integration of the piece-wise linear PSD profile of Figure 16 over bandwidths of 5 MHz centred on adjacent 5 MHz channels results in the terminal station ACLR values presented in Table 7.

Table 7: Terminal station ACLRs required for compliance with the SE42 BEM, assuming a piece-wise linear radiation PSD profile and radiation at the maximum in-block EIRP of 31 dBm/(5 MHz).

ACLR (dB)	n th adjacent channel			
	n = 1	n = 2	n = 3	n = 4
	33	45	54	63

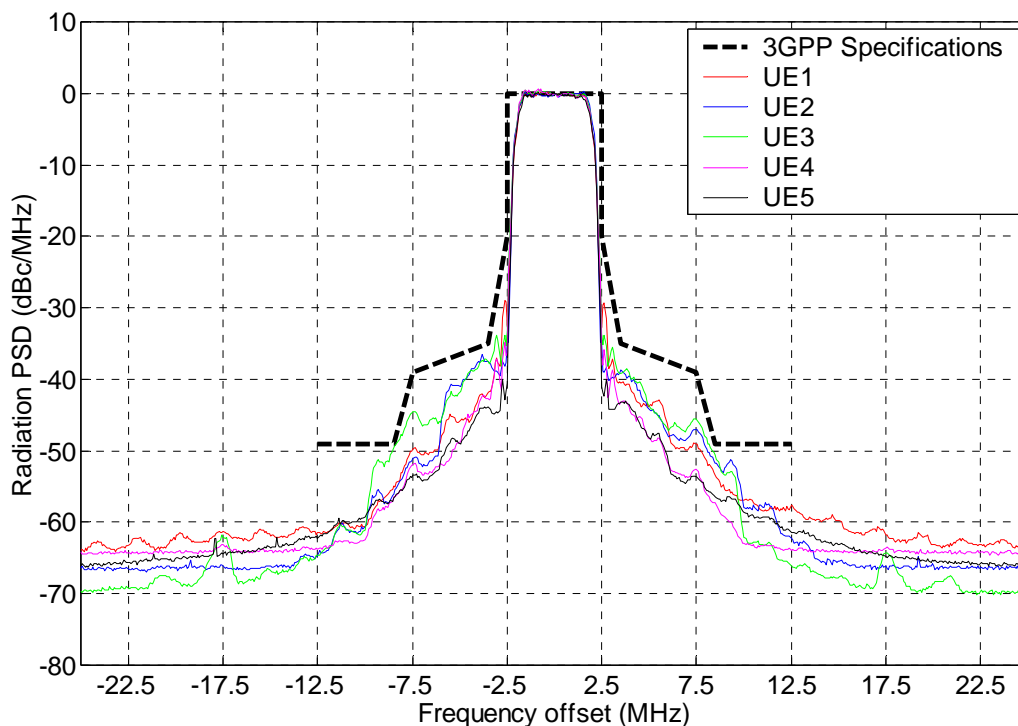
- A2.11 Note that the above ACLR values for the 1st and 2nd adjacent 5 MHz channels are similar to the corresponding ACLR minimum requirements of 33 and 43 dB specified in 3GPP TS 25.101 for UTRA-FDD user equipment.
- A2.12 While more elaborate PSD profiles³¹ can be formulated to more precisely model the characteristics of terminal station radiation, we believe that the simple PSD profile presented above adequately captures realistic levels of spectral leakage in the first few critical adjacent channels.
- A2.13 We have assumed the ACLR values of Table 7 in the derivation of the results presented in Section 4 of this document for the case of terminal stations served by TDD macro-cells, and with their in-block EIRP limited to a maximum value of 31 dBm/(5 MHz). Note that this is a conservative assumption, since, unless it is located at the cell-edge, a terminal station is likely to transmit at less than the maximum permitted EIRP of 31 dBm/(5 MHz), and would therefore be associated with greater ACLR values than those shown in Table 7.

³¹ One example would be to apply an appropriate lower-bound on the radiation PSD at frequency offsets beyond a certain threshold in order to account for phenomena such as spurious emissions.

Spectral leakage with terminal stations operating at less than the maximum permitted EIRP

- A2.14 The ACLR values presented in the previous sub-section correspond to the case where a terminal station complies with the SE42 BEM while operating at the maximum in-block mean EIRP level permitted by the regulatory technical conditions (as might be the case when the terminal is located at the edge of a macro-cell).
- A2.15 However, spectral leakage typically reduces with respect to the in-block EIRP when a terminal station radiates at less than full power (as might be the case when the terminal is located close to the serving base station). This is because the terminal station's power amplifier is not driven into saturation in such circumstances and is therefore able to generate a less distorted (and hence more spectrally pure) signal.
- A2.16 This is indeed confirmed by inspection of Figure 17 which shows measured³² radiation PSDs of commercially available UTRA-FDD UEs in the 2.1 GHz band. Results are presented for UEs belonging to five different manufacturers and for an EIRP of 20 dBm/(3.84 MHz). Also shown, is the minimum (relative) requirement on the spectrum emission mask of a UE as specified in 3GPP TS 25.101. For clarity, all relative power levels are normalised to dBc/MHz. Frequency offset is with respect to the carrier.

Figure 17: Measured radiation PSDs of UTRA-FDD UEs in the 2.1 GHz band belonging to five different manufacturers. EIRP is 20 dBm/(3.84 MHz).



³² The measurements were performed by a spectrum analyser at a frequency resolution of 80 kHz and with a measurement bandwidth of 18 kHz. The results were then normalised to correspond to a measurement bandwidth of 1 MHz, and finally compared to the carrier power measured over 3.84 MHz.

A2.17 The corresponding out-of-channel emission levels are presented in Table 8. These are derived by the numerical integration of the PSDs in Figure 17 over bandwidths of 3.84 MHz centred on adjacent 5 MHz channels, averaged over positive and negative frequency offsets, and averaged over all five UEs.

Table 8: Measured spectral leakage of UTRA-FDD UEs in the 2.1 GHz band. EIRP is 20 dBm/(3.84 MHz).

Out-of-channel emission (dBc/MHz)	n th adjacent channel			
	n = 1	n = 2	n = 3	n = 4
3GPP	-35.7	-48.7	-49.0	-49.0
Measured	-43.5	-56.1	-63.4	-65.0

A2.18 The results indicate that the spectral leakage is lower than the minimum requirements specified in 3GPP TS 25.101 by around 8 dB at the 1st adjacent channel, by around 7 dB at the 2nd adjacent channel, and by more than 10 dB at greater frequency offsets.

A2.19 The above margins are also broadly confirmed through the direct measurement of radiation ACLR for the five UEs. These results, provided by the ACLR measurement functionalities of a commercial wireless communications test set, are summarised in Table 9.

Table 9: Measured ACLR of UTRA-FDD UEs in the 2.1 GHz band belonging to five different manufacturers. EIRP is 20 dBm/(3.84 MHz).

Frequency offset (MHz)	ACLR (dB)					
	3GPP (TS 25.101)	UE 1	UE 2	UE 3	UE 4	UE 5
-10	43	51.3	48.9	49.6	45.1	45.9
-5	33	42.2	39.2	37.7	42.4	43.0
+5	33	41.6	42.8	40.4	42.2	42.5
+10	43	50.8	48.8	50.7	45.2	46.0

A2.20 The above results indicate that, averaged over all five UEs, the radiation ACLRs are 8 to 9 dB greater in the 1st adjacent channel (± 5 MHz offset) and 5 to 6 dB greater in the 2nd adjacent channel (± 10 MHz offset), as compared with the corresponding ACLR minimum requirements specified in 3GPP TS 25.101.

A2.21 Based on the above, we infer that a terminal station which operates at levels well below the maximum permitted in-block mean EIRP of 31 dBm/(5 MHz) in the 2.6 GHz band can be characterised by ACLRs that are greater than those implied by the SE42 BEM by around 8 dB at the 1st adjacent channel, by around 5 dB at the 2nd adjacent channel, and by 10 dB at greater frequency offsets (i.e., ACLRs of 41, 50, 64, and 73 dB respectively).

A2.22 Based on the above, we have assumed the ACLR values of 41, 50, 64, and 73 dB at the 1st, 2nd, 3rd, and 4th adjacent channels in the derivation of the results presented in Section 4 of this document for the case of terminal stations served by TDD pico-cells, and with their EIRP limited to a maximum value of 25 dBm/(5 MHz).

Conclusions

- A2.1 We have shown, based on a piece-wise linear model for the radiation PSD of a terminal station in the 2.6 GHz band, that compliance with the SE42 BEM implies ACLRs of 33, 45, 54, and 63 dB at the 1st, 2nd, 3rd, and 4th adjacent (5 MHz) blocks respectively. Here it was assumed that the terminal station operates at the maximum permitted in-block mean EIRP of 31 dBm/(5 MHz). These ACLR values are used in the analysis presented in Section 4 of this document to characterise terminal stations which are served by TDD macro-cells.
- A2.2 We have further shown, based on measurements of the spectral leakage of UTRA-FDD UE radiation in the 2.1 GHz band, and their comparison with the 3GPP minimum requirements, that terminal stations which operate at levels well below the maximum permitted in-block mean EIRP in the 2.6 GHz band can be characterised by ACLRs of 41, 50, 64, and 73 dB at the 1st, 2nd, 3rd, and 4th adjacent (5 MHz) blocks respectively. These ACLR values are used in the analysis presented in Section 4 of this document to characterise terminal stations which are served by TDD pico-cells, and with their EIRP limited to a maximum value of 25 dBm/(5 MHz).

Annex 3

Terminal station receiver performance

- A3.1 In this annex we quantify the potential for frequency discrimination by terminal station receivers in the 2.6 GHz band.
- A3.2 We first describe a methodology for computing the adjacent-channel selectivity (ACS) of a terminal station based on measurements of its receiver characteristics. We subsequently present commissioned measurements³³ of commercially available UTRA-FDD user equipment (UE) operating in the 2.1 GHz band. These measurements are used to evaluate realistic levels of a) ACS, b) saturation performance, and c) inter-modulation performance, as exhibited by the type of terminal station equipment which might be deployed in the 2.6 GHz band.
- A3.3 The derived results are used (along with the ACLR values derived in Annex 2) in the analysis presented in Section 4 of this document to examine the impact of terminal-to-terminal interference in the 2.6 GHz band.
- A3.4 Unless otherwise stated, all signal power measurements are made at the output of a root-raised cosine filter of bandwidth 3.84 MHz and with a roll-off factor of 0.22.

Methodology for computing ACS

- A3.5 The ACS of a receiver is defined as the ratio of the receiver's filter attenuation over its pass-band divided by the receiver's filter attenuation over an adjacent frequency channel.
- A3.6 Furthermore, as described in Annex 2, the adjacent-channel leakage ratio (ACLR) of a signal is defined as the ratio of the signal's power (nominally equal to the power over the signal's pass-band) divided by the power of the signal when measured at the output of a (nominally rectangular) receiver filter centred on an adjacent frequency channel.
- A3.7 It is evident that the level of interference experienced by a receiver as a result of the presence of an adjacent-channel interferer is a function of both the interferer's finite ACLR and the receiver's finite ACS. By defining the adjacent-channel interference ratio (ACIR) as the ratio of the power, P_{AC} , of an adjacent-channel interferer received at the terminal station, divided by the interference power, P_I , experienced by the victim receiver, one may write³⁴

$$ACIR = \frac{P_{AC}}{P_I} = \left(ACLR^{-1} + ACS^{-1} \right)^{-1}, \quad (22)$$

³³ ERA Technology, "Measurements of UTRA-FDD user equipment characteristics in the 2.1 GHz band," final report, April 2008. Document is available at: <http://www.ofcom.org.uk/consult/condocs/2ghzregsnotice/>.

³⁴ Note that this excludes the minor contribution to interference caused by the spectral overlap between the receive filter's frequency response and the power spectral density of the interferer over those frequencies which fall outside the pass-bands of the receive filter and interferer.

or equivalently that,

$$\text{ACS} = \left(\left(\frac{P_{\text{AC}}}{P_{\text{I}}} \right)^{-1} - \text{ACLR}^{-1} \right)^{-1}. \quad (23)$$

A3.8 Equation 23 describes how a terminal station receiver's ACS can be computed based on measurements of the power, P_{AC} , of an adjacent-channel test interferer received at the terminal station, the test interferer's ACLR, and the effective interference power, P_{I} , experienced by the terminal station receiver. However, the latter parameter can not be observed directly, and will therefore need to be measured indirectly, for example via the procedure described next.

A3.9 Consider a test scenario where a terminal station receives a wanted downlink signal at a power level P_{S} . Let the introduction at the receiver of an adjacent-channel test interferer of power P_{AC} , with an adjacent-channel leakage ratio, ACLR, result in a bit error probability of P_{e} . Then, let the adjacent-channel interferer be replaced by a co-channel test interferer received at power P_{CC} , such that the bit-error rate remains fixed at P_{e} . The unchanged bit error probability would imply that the signal-to-interference-plus-noise ratio (SINR) is the same in the two scenarios. Assuming that the receiver's noise figure is also unchanged in the two scenarios, and using P_{N} to denote the thermal noise-floor of the receiver, we may write,

$$\text{SINR} = \frac{P_{\text{S}}}{P_{\text{N}} + P_{\text{CC}}} = \frac{P_{\text{S}}}{P_{\text{N}} + P_{\text{I}}}, \quad (24)$$

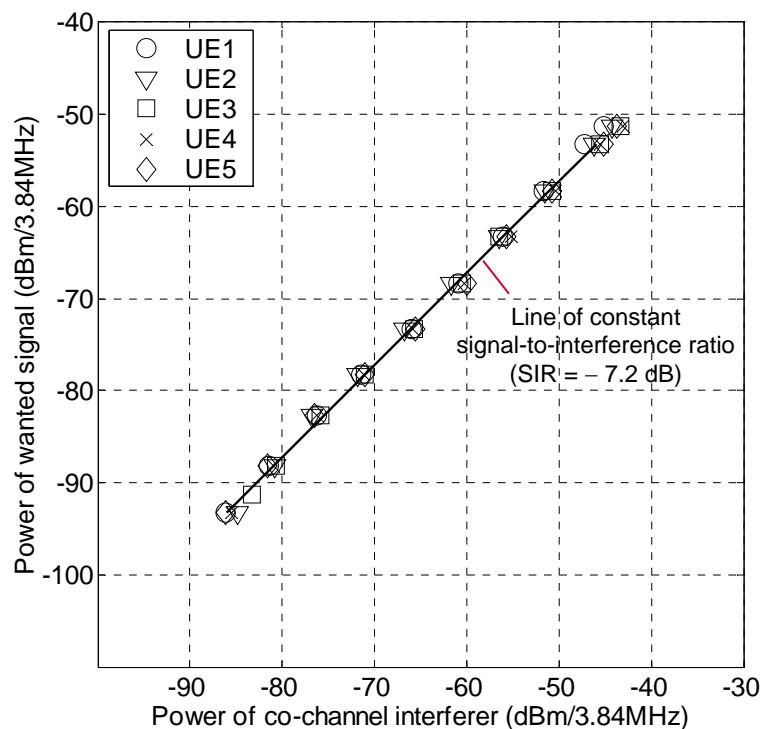
or simply that, $P_{\text{I}} = P_{\text{CC}}$. In other words, the power level of the co-channel test interferer provides an indication of the level of interference the receiver experiences in the presence of an adjacent-channel test interferer.

A3.10 The above methodology is used in the following sub-sections to derive ACS values based on over-the-air measurements of P_{CC} , P_{S} , P_{AC} , and ACLR for a number of UTRA-FDD UEs operating in the 2.1 GHz band. Details of the test set-up and measurement equipment are available in the report by ERA Technology³³.

Measurements of UE receiver performance with a co-channel interferer

- A3.11 Figure 18 shows the measurements at the UE of the received power, P_S , of a wanted downlink signal as a function of the received power, P_{CC} , of a co-channel test interferer, for a fixed bit-error probability of 10^{-3} . Results are presented for five different UEs.
- A3.12 The wanted signal is a WCDMA signal as defined in the relevant 3GPP test specifications, whose power, P_S , is equivalent to the 3GPP parameter \hat{I}_{or} . The co-channel test interferer is a white noise signal whose power, P_{CC} , is measured over a bandwidth of 3.84 MHz centred on the wanted signal carrier.

Figure 18: Measurements of UE receiver performance in the presence of a co-channel interferer, and for a bit-error rate of 10^{-3} .



- A3.13 Averaging over all measurement points, one may observe that the bit-error probability of 10^{-3} is achieved at a co-channel signal-to-interference ratio of

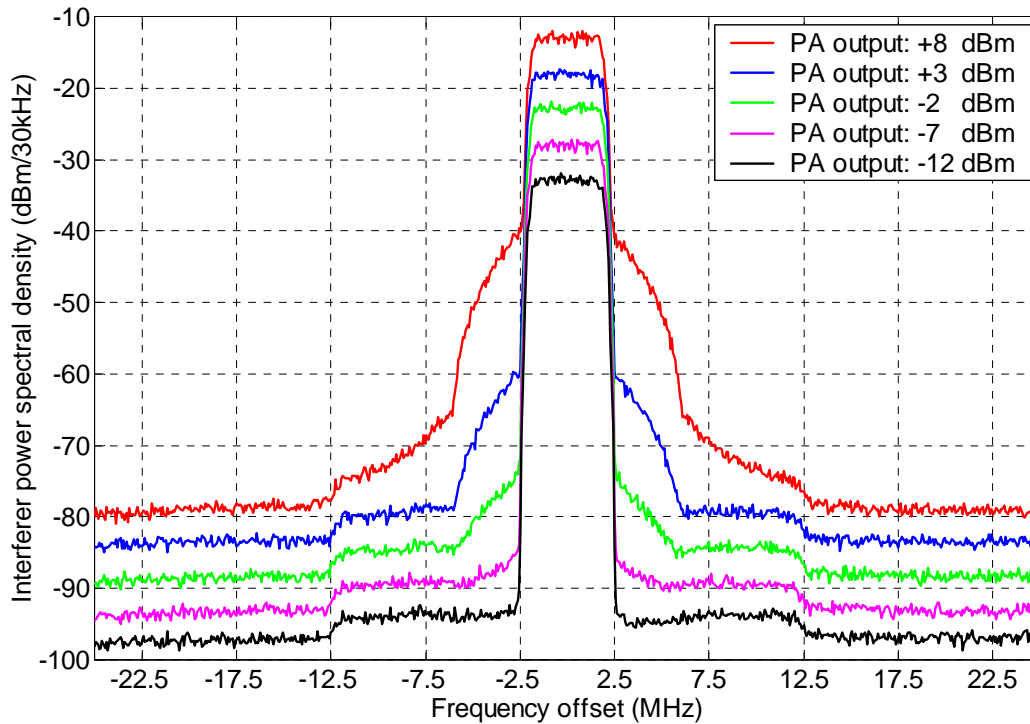
$$\text{SIR} = \frac{P_S}{P_{CC}} \equiv -7.2 \text{ dB}, \quad (25)$$

as identified by the solid line in Figure 18. The above measured values of P_{CC} will be used to represent the interference power levels, P_I , experienced by a UE receiver when suffering from the same bit-error probability of 10^{-3} in the presence of adjacent-channel test interferers.

Measurements of test interferer ACLR

A3.14 Figure 19 illustrates the measured power spectral density (PSD) of the adjacent-channel test interferer at the output of a power amplifier prior to radiation over the air, and for a number of different interferer signal power levels.

Figure 19: Measurements of adjacent-channel interferer PSD.



A3.15 The following conclusions may be drawn:

- The ACLR of the test interferer signal decreases with increasing power levels of the interferer. This is due to the non-linear behaviour of the power amplifier when it is driven into saturation in order to generate high power levels at its output.
- The decrease in the test interferer ACLR due to power amplifier saturation is most evident at the 1st and 2nd adjacent channels.
- The test interferer ACLRs at the 3rd and 4th adjacent channels are not significantly affected by the saturation of the power amplifier.
- Averaged over positive and negative frequency offsets, and with the PSDs numerically integrated over bandwidths of 3.84 MHz, the test interferer ACLRs are seen to be (35, 49, 57, 61, 61) dB in the 1st adjacent channel, and (60, 61, 61, 61, 61) dB in the 2nd adjacent channel, for power amplifier outputs of (8, 3, -2, -7, -12) dBm/(3.84 MHz) respectively. In other words, when the power amplifier is not driven into saturation, the interferer ACLRs at the 1st and 2nd adjacent channels are more or less equal, and are of the order of 61 dB.
- Averaged over positive and negative frequency offsets, and with the PSDs numerically integrated over bandwidths of 3.84 MHz, the interferer ACLRs are

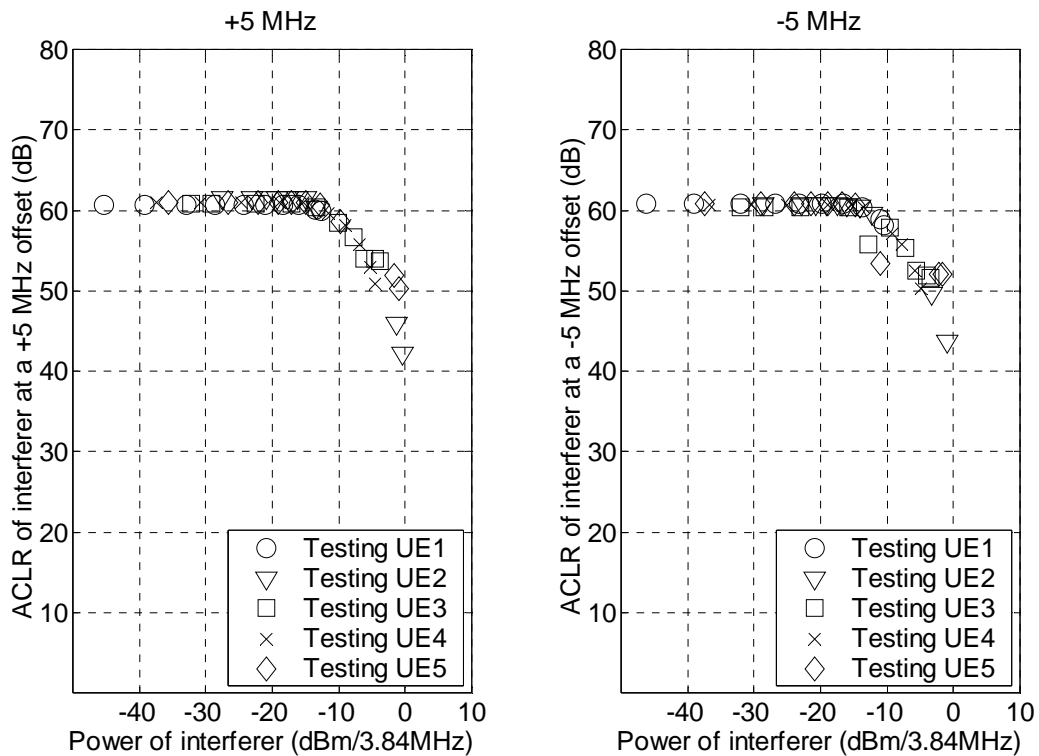
seen to be (65, 65, 65, 65, 64) dB for the 3rd adjacent channel, and (66, 65, 65, 65, 64) dB for the 4th adjacent channel, for power amplifier outputs of (8, 3, -2, -7, -12) dBm/(3.84 MHz) respectively. In other words, whether the power amplifier is driven into saturation or not, the interferer ACLRs at the 3rd and 4th adjacent channels are more or less equal, and are of the order of between 64 and 65 dB.

A3.16 Specific values of test interferer ACLR measured during the testing of the different UEs are presented next.

a) Measurements of interferer ACLR at the 1st adjacent channels (± 5 MHz)

A3.17 Figure 20 shows measurements³⁵ of the interferer ACLR for frequency offsets of +5 and -5 MHz respectively from its carrier frequency, as a function of the power, P_{AC} , of the interferer received at the UE. Results are presented as measured during the testing of five different UE receivers.

Figure 20: Measured test interferer ACLR at the 1st adjacent channel (± 5 MHz).



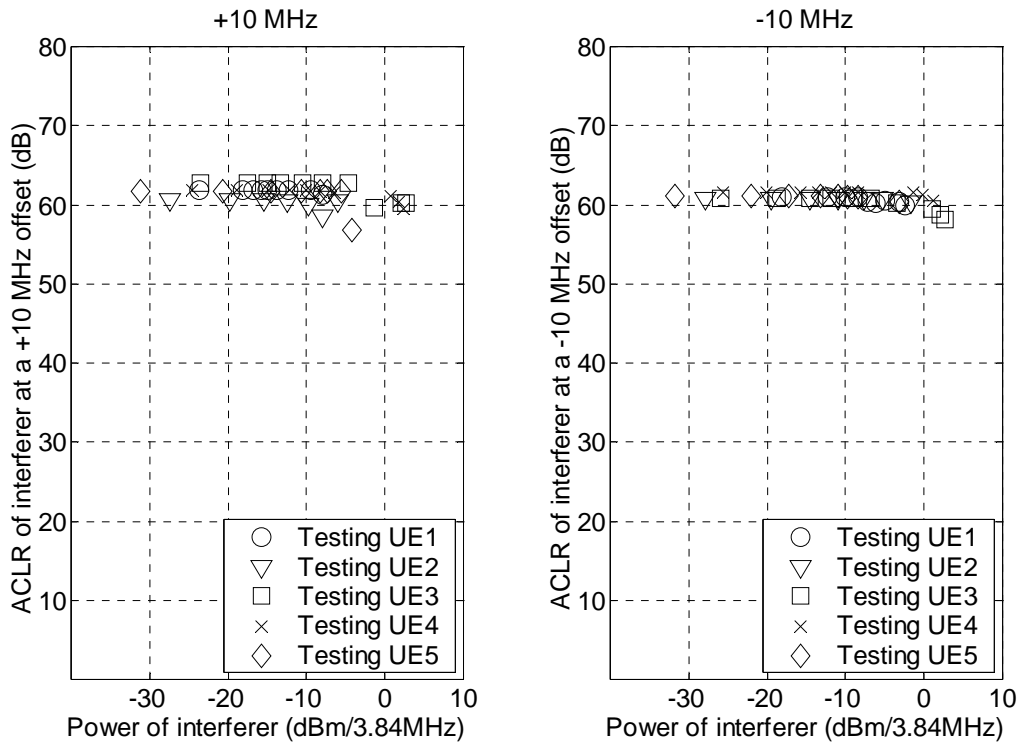
A3.18 As can be seen, the variation of interferer ACLR with interferer power is broadly the same during the testing of the different UEs. The interferer ACLR settles at around 61 dB for $P_{AC} < -15$ dBm/(3.84 MHz).

³⁵ In the measurements performed by ERA Technology, the measured interferer ACLR can be seen to anomalously decrease (rather than increase, or at least remain fixed) with a reduction in interferer power. The observed rate of reduction suggests that this phenomenon was due to the employed spectrum analyser being unable to measure the interferer power that is leaked into the adjacent channel when this fell below the analyser's noise-floor for low interferer power levels. This has been corrected in the results presented in this document by maintaining the ACLR at its peak value with a reduction in interferer power.

b) Measurements of interferer ACLR at the 2nd adjacent channels (± 10 MHz)

A3.19 Figure 21 shows measurements³⁵ of the interferer ACLR for frequency offsets of +10 and -10 MHz respectively from its carrier frequency, as a function of the power, P_{AC} , of the interferer received at the UE. Results are presented as measured during the testing of five different UE receivers.

Figure 21: Measured test interferer ACLR at the 2nd adjacent channel (± 10 MHz).



A3.20 Again, the variation of interferer ACLR with interferer power is broadly the same during the testing of the different UEs (less so for case of +10 MHz offset). The interferer ACLR settles at around 61 dB for $P_{AC} < -15$ dBm/(3.84 MHz).

c) Measurements of interferer ACLR at the 3rd adjacent channels (± 15 MHz)

A3.21 No detailed measurements of interferer ACLR were undertaken for frequency offsets of ± 15 MHz. However, an inspection of the interferer PSDs that were illustrated in Figure 19 indicates an ACLR of between 64 and 65 dB at the 3rd adjacent channel. Moreover, this ACLR was seen to be somewhat insensitive with respect to the saturation of the power amplifier.

A3.22 For the purposes of this study, we will assume an overestimated interferer ACLR of 65 dB at the 3rd and 4th adjacent channels, with the understanding that this would result in an underestimation of the UE receiver ACS (see Equation 23) in the calculations of the following sub-sections.

Measurements of UE receiver ACS

a) Measurements of UE ACS at the 1st adjacent channels (± 5 MHz)

A3.23 Figure 22 and Figure 23 show measurements at the UE of the received power, P_S , of a wanted downlink signal as a function of the received power, P_{AC} , of an interferer at the 1st adjacent channel, and for a constant bit-error probability of 10^{-3} . Results are presented for five different UEs and for carrier-to-carrier frequency offsets of +5 and –5 MHz between the wanted signal and interferer. Also shown are the minimum requirements for the above parameters as specified in 3GPP TS 25.101.

A3.24 Figure 24 and Figure 25 show the computed values of UE receiver ACS as a function of the received power, P_{AC} , of an interferer at the 1st adjacent channel. These are computed in accordance with Equation 23, using the relevant values of P_{AC} , P_I (namely P_{CC}), and test interferer ACLR presented in Figure 18 and Figure 20.

A3.25 The following observations can be made:

- When averaged across all tested UEs, the measurements indicate a UE receiver ACS of around 53 dB for interferer power levels of up to –25 dBm/(3.84 MHz) at the 1st adjacent channel.
- There is generally a reduction in the UE receiver ACS for interferer power levels greater than –25 dBm/(3.84 MHz) at the 1st adjacent channel. This is due to the onset of non-linear behaviour within the UE receiver chain, which results in a greater than proportional increase in the levels of experienced interference for an increase in interferer power.
- When averaged across all tested UEs, the measurements indicate that a UE receiver ACS of 33 dB can be achieved for interferer power levels of up to –10 dBm/(3.84 MHz) or greater. This is to be compared with a 3GPP minimum requirement for an ACS of 33 dB³⁶ with an interferer power level of –25 dBm/(3.84 MHz) at the 1st adjacent channel.

A3.26 Based on the above observations, we have assumed an ACS of 53 dB at the 1st adjacent channel, and a saturation interferer power threshold, Π_{Sat} , of –10 dBm, in the derivation of the results presented in Section 4 of this document (as also described in Annex 1).

³⁶ 3GPP TS 25.101 directly specifies a minimum ACS of 33 dB at the 1st adjacent channel (± 5 MHz). 3GPP TS 25.101 also specifies ACS indirectly by requiring that a terminal station is desensitised by no more than 14 (or 41) dB with respect to reference sensitivity performance, when subjected to a test interferer power of –52 (or –25) dBm/(3.84 MHz) received in the 1st adjacent channel. The indirect specification can be interpreted as described next. Assuming a terminal station receiver noise figure of 9 dB, the thermal noise floor can be computed to be $kTBNF = -99$ dBm/(3.84 MHz). The desensitisation of 14 (or 41) dB implies that the interference experienced by the receiver is –85 (or –58) dBm/(3.84 MHz), which when compared to the specified interferer power of –52 (or –25) dBm/(3.84 MHz), implies an ACIR or 33 dB. Finally, if the ACLR of the test interferer is significantly greater than the ACIR, then $ACS \approx ACIR = 33$ dB. In other words, the direct and indirect specifications are consistent.

Figure 22: Measured variation of P_s versus P_{AC} for UEs in the presence of an interferer at the 1st adjacent channel (+5 MHz), and for a DL bit-error rate of 10^{-3} .

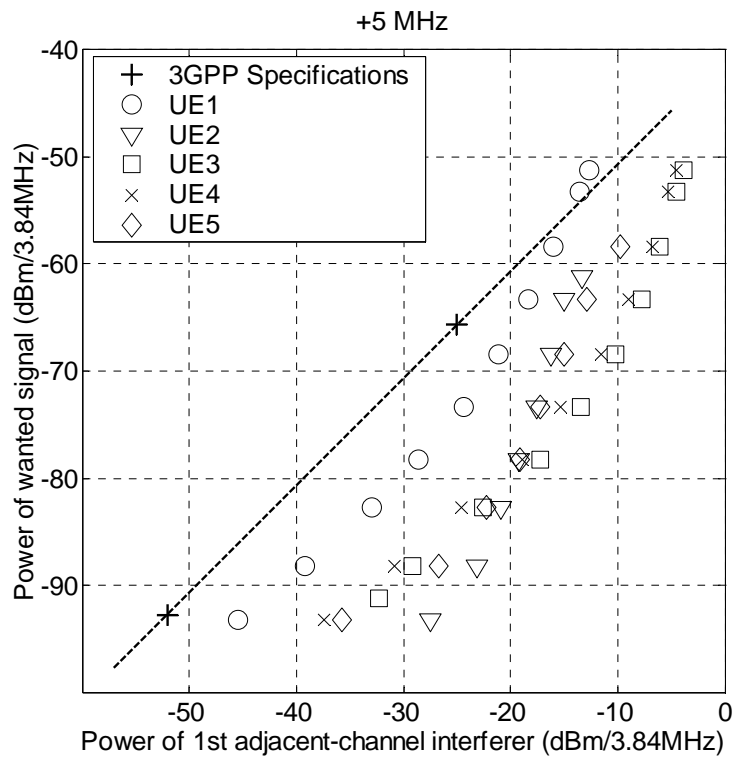


Figure 23: Measured variation of P_s versus P_{AC} for UEs in the presence of an interferer at the 1st adjacent channel (-5 MHz), and for a DL bit-error rate of 10^{-3} .

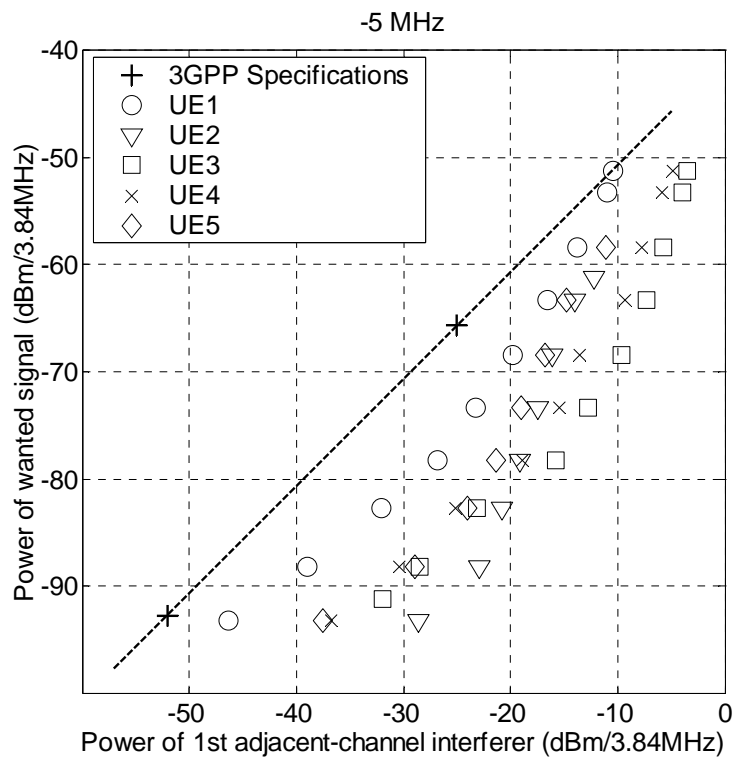


Figure 24: UE ACS at the 1st adjacent channel (+5 MHz).

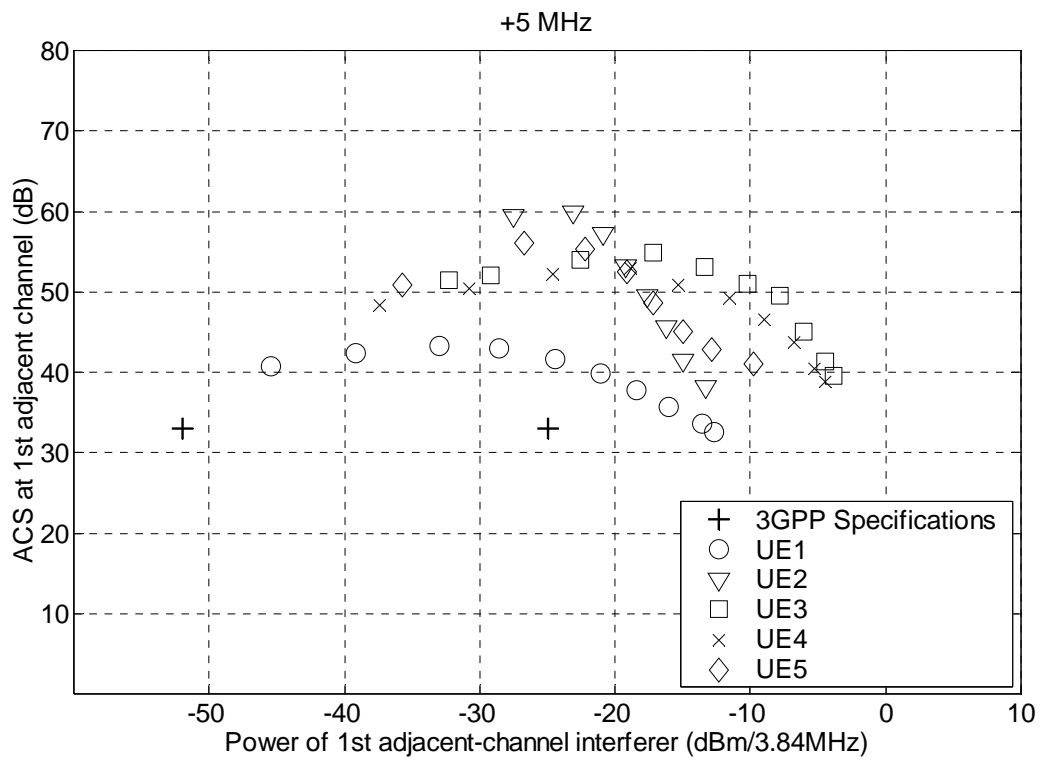
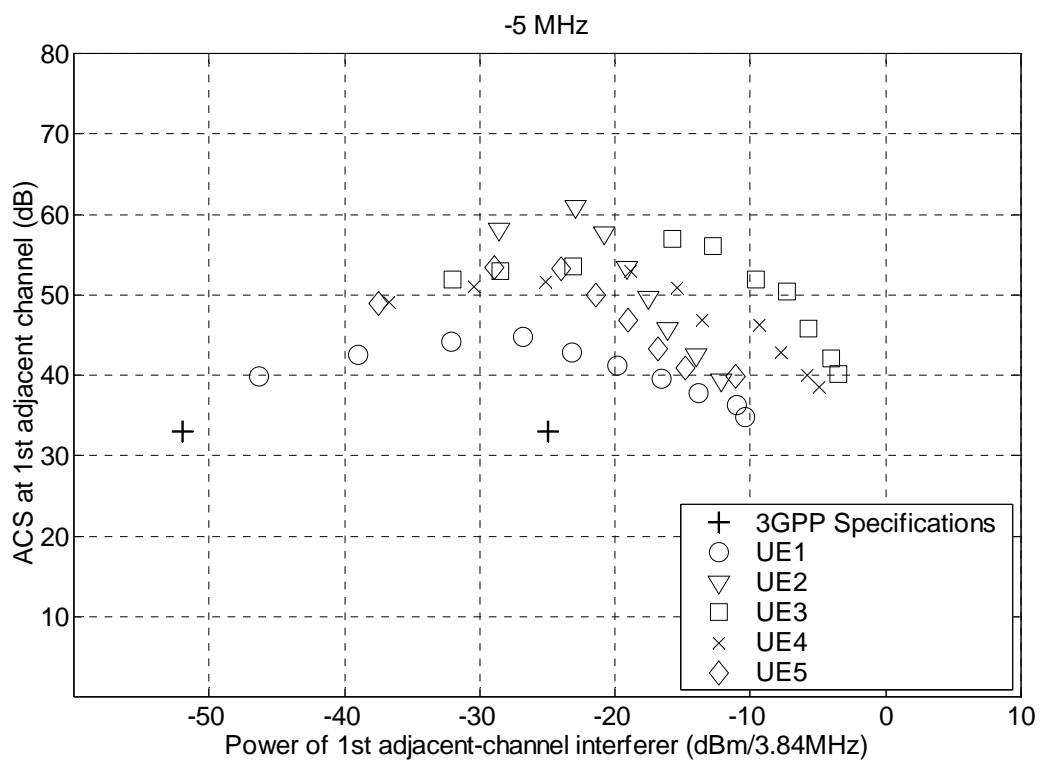


Figure 25: UE ACS at the 1st adjacent channel (-5 MHz).



b) Measurements of UE ACS at the 2nd adjacent channels (± 10 MHz)

A3.27 Figure 26 and Figure 27 show measurements at the UE of the received power, P_S , of a wanted downlink signal as a function of the received power, P_{AC} , of an interferer at the 2nd adjacent channel, and for a constant bit-error probability of 10^{-3} . Results are presented for five different UEs and for carrier-to-carrier frequency offsets of +10 and –10 MHz between the wanted signal and interferer. Also shown are the minimum requirements for the above parameters as specified in 3GPP TS 25.101.

A3.28 Figure 28 and Figure 29 show the computed values of UE receiver ACS as a function of the received power, P_{AC} , of an interferer at the 2nd adjacent channel. These are computed³⁷ in accordance with Equation 23, using the relevant values of P_{AC} , P_I (namely P_{CC}), and test interferer ACLR presented in Figure 18 and Figure 21.

A3.29 The following observations can be made:

- When averaged across all tested UEs, the measurements indicate a UE receiver ACS of around 65 dB for interferer power levels of up to –15 dBm/(3.84 MHz) at the 2nd adjacent channel.
- There is generally a reduction in the UE receiver ACS for interferer power levels greater than –15 dBm/(3.84 MHz) at the 2nd adjacent channel, again due to the onset of non-linear behaviour within the UE receiver chain.
- When averaged across all tested UEs, the measurements indicate that a UE receiver ACS of 43 dB can be achieved for interferer power levels of up to 0 dBm/(3.84 MHz) or greater. This is to be compared with a 3GPP minimum requirement for an ACS of 43 dB³⁸ with an interferer power level of –56 dBm/(3.84 MHz) at the 2nd adjacent channel.

A1.2 Based on the above observations, we have assumed an ACS of 65 dB at the 2nd adjacent channel in the derivation of the results presented in Section 4 of this document (as also described in Annex 1).

³⁷ In order to avoid overestimation of the ACS values, we have not included in our calculations those few measurement points where the interferer ACLR is less than 0.5 dB greater than the ACIR.

³⁸ 3GPP TS 25.101 specifies blocking performance by requiring that a terminal station is desensitised by no more than 3 dB with respect to reference sensitivity performance, when subjected to a test interferer power of –56 dBm/(3.84 MHz) received in the 2nd adjacent channel (± 10 MHz).

Assuming a terminal station receiver noise figure of 9 dB, the thermal noise floor can be computed to be $kTBNF = -99$ dBm/(3.84 MHz). The desensitisation of 3 dB implies that the interference experienced by the receiver is also –99 dBm/(3.84 MHz), which when compared to the specified interferer power of –56 dBm/(3.84 MHz), implies an ACIR or 43 dB. Finally, if the ACLR of the test interferer is significantly greater than the ACIR (as implied in TS 25.101), then $ACS \approx ACIR = 43$ dB.

Figure 26: Measured variation of P_s versus P_{AC} for UEs in the presence of an interferer at the 2nd adjacent channel (+10 MHz) and for a DL bit-error rate of 10^{-3} .

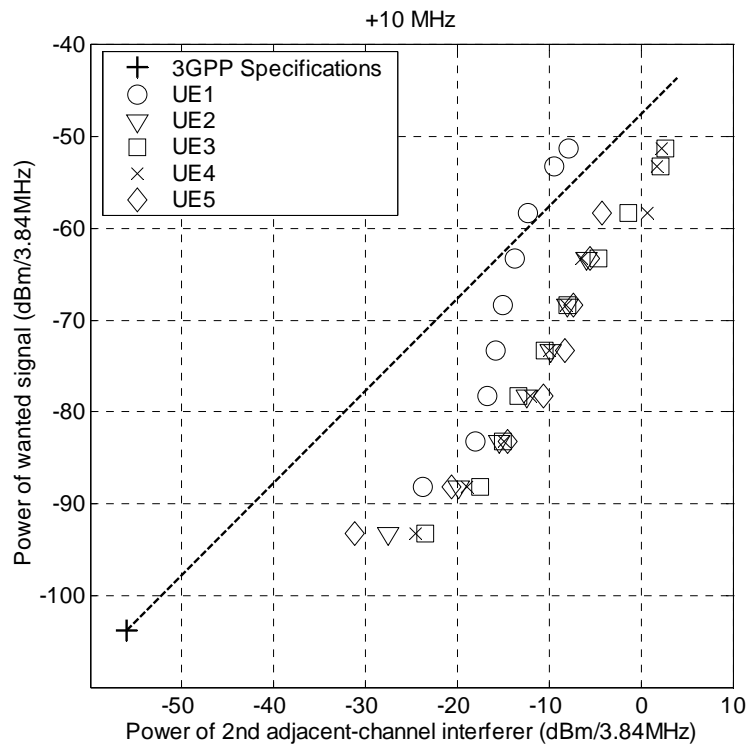


Figure 27: Measured variation of P_s versus P_{AC} for UEs in the presence of an interferer at the 2nd adjacent channel (-10 MHz) and for a DL bit-error rate of 10^{-3} .

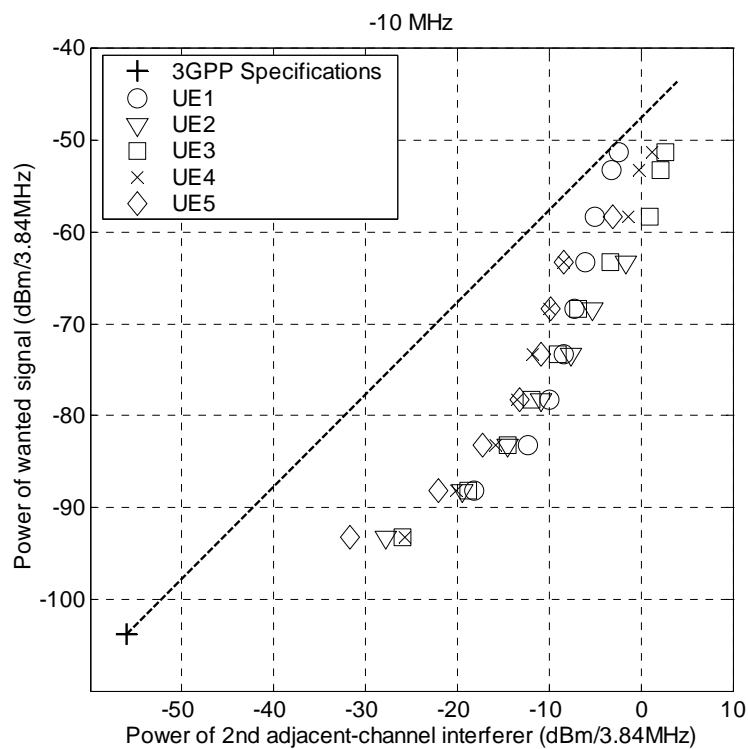


Figure 28: UE ACS at the 2nd adjacent channel (+10 MHz).

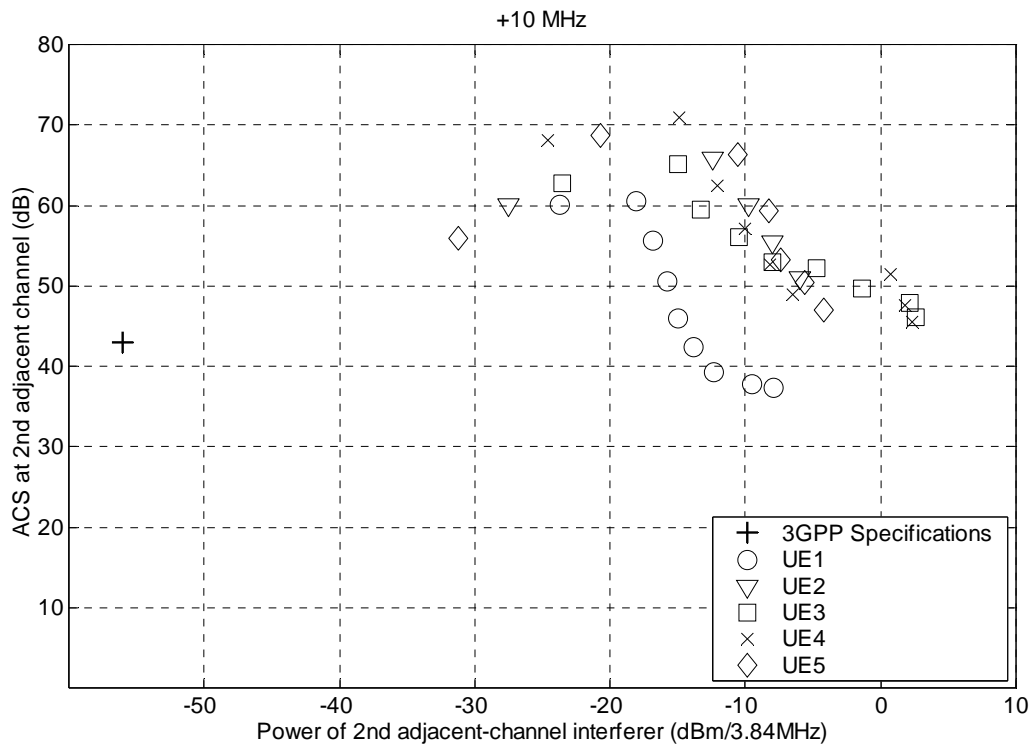
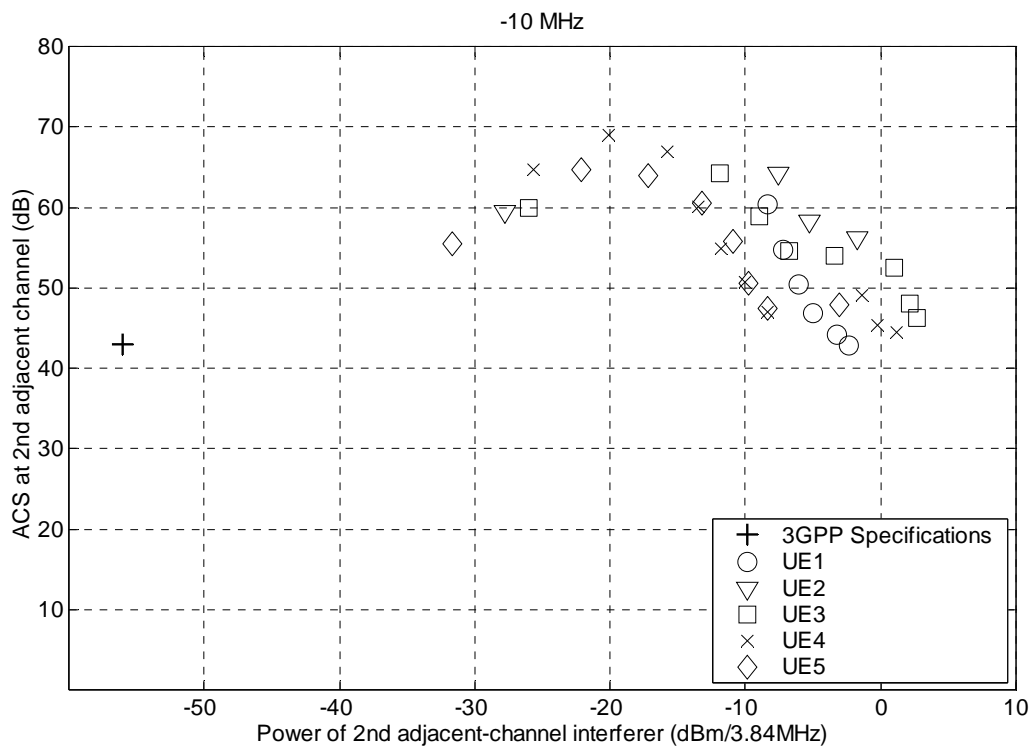


Figure 29: UE ACS at the 2nd adjacent channel (-10 MHz).



c) Measurements of UE ACS at the 3rd adjacent channels (± 15 MHz)

A3.30 Figure 30 and Figure 31 show measurements at the UE of the received power, P_S , of a wanted downlink signal as a function of the received power, P_{ACI} , of an interferer at the 3rd adjacent channel, and for a constant bit-error probability of 10^{-3} . Results are presented for five different UEs and for carrier-to-carrier frequency offsets of +15 and -15 MHz between the wanted signal and interferer. Also shown are the minimum requirements for the above parameters as specified in 3GPP TS 25.101.

A3.31 Figure 32 and Figure 33 show the computed values of UE receiver ACS as a function of the received power, P_{AC} , of an interferer at the 3rd adjacent channel. These are computed³⁷ in accordance with Equation 23, using the relevant values of P_{AC} , P_I (namely P_{CC}), and interferer ACLR presented in Figure 18 and Figure 19.

A3.32 The following observations can be made:

- When averaged across all tested UEs, the measurements indicate a UE receiver ACS of around 70 dB for interferer power levels of up to -15 dBm/(3.84 MHz) at the 3rd adjacent channel.
- There is generally a reduction in the UE receiver ACS for interferer power levels greater than -15 dBm/(3.84 MHz) in the 3rd adjacent channel, again due to the onset of non-linear behaviour within the UE receiver chain.
- When averaged across all tested UEs, the measurements indicate that a UE receiver ACS of 55 dB can be achieved for interferer power levels of up to -5 dBm/(3.84 MHz) or greater. This is to be compared with a 3GPP minimum requirement for an ACS of 55 dB³⁹ with an interferer power level of -44 dBm/(3.84 MHz) at the 3rd adjacent channel.

A3.33 Based on the above observations, we have assumed an (conservative) ACS of 65 dB at the 3rd (and 4th) adjacent channel in the derivation of the results presented in Section 4 of this document (as also described in Annex 1).

³⁹ 3GPP TS 25.101 specifies blocking performance by requiring that a terminal station is desensitised by no more than 3 dB with respect to reference sensitivity performance, when subjected to a test interferer power of -44 dBm/(3.84 MHz) received in the 3rd adjacent channel (± 15 MHz).

Assuming a terminal station receiver noise figure of 9 dB, the thermal noise floor can be computed to be $kTBNF = -99$ dBm/(3.84 MHz). The desensitisation of 3 dB implies that the interference experienced by the receiver is also -99 dBm/(3.84 MHz), which when compared to the specified interferer power of -44 dBm/(3.84 MHz), implies an ACIR or 55 dB. Finally, if the ACLR of the test interferer is significantly greater than the ACIR (as implied in TS 25.101), then $ACS \approx ACIR = 55$ dB.

Figure 30: Measured variation of P_s versus P_{AC} for UEs in the presence of an interferer at the 3rd adjacent channel (+15 MHz) and for a DL bit-error rate of 10^{-3} .

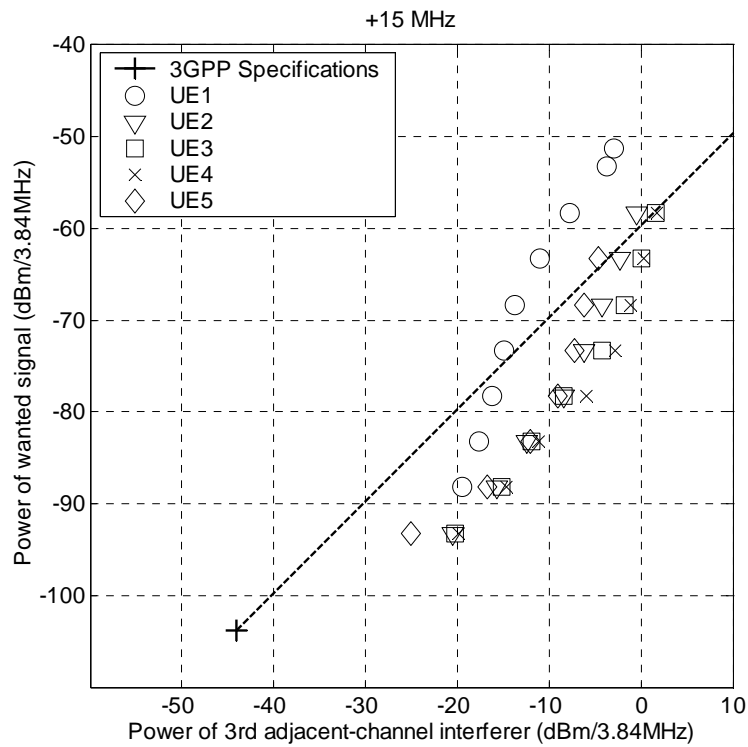


Figure 31: Measured variation of P_s versus P_{AC} for UEs in the presence of an interferer at the 3rd adjacent channel (-15 MHz) and for a DL bit-error rate of 10^{-3} .

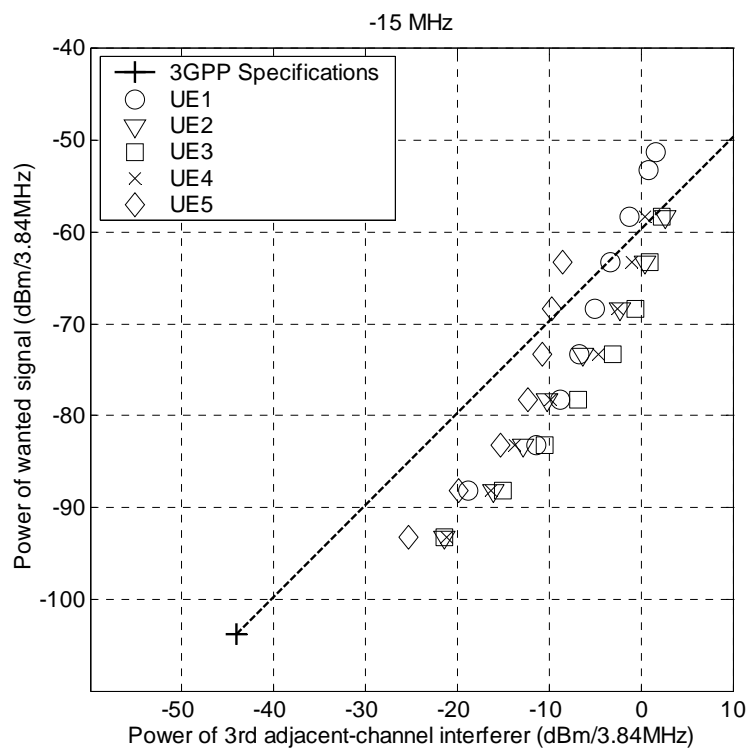


Figure 32: UE ACS at the 3rd adjacent channel (+15 MHz).

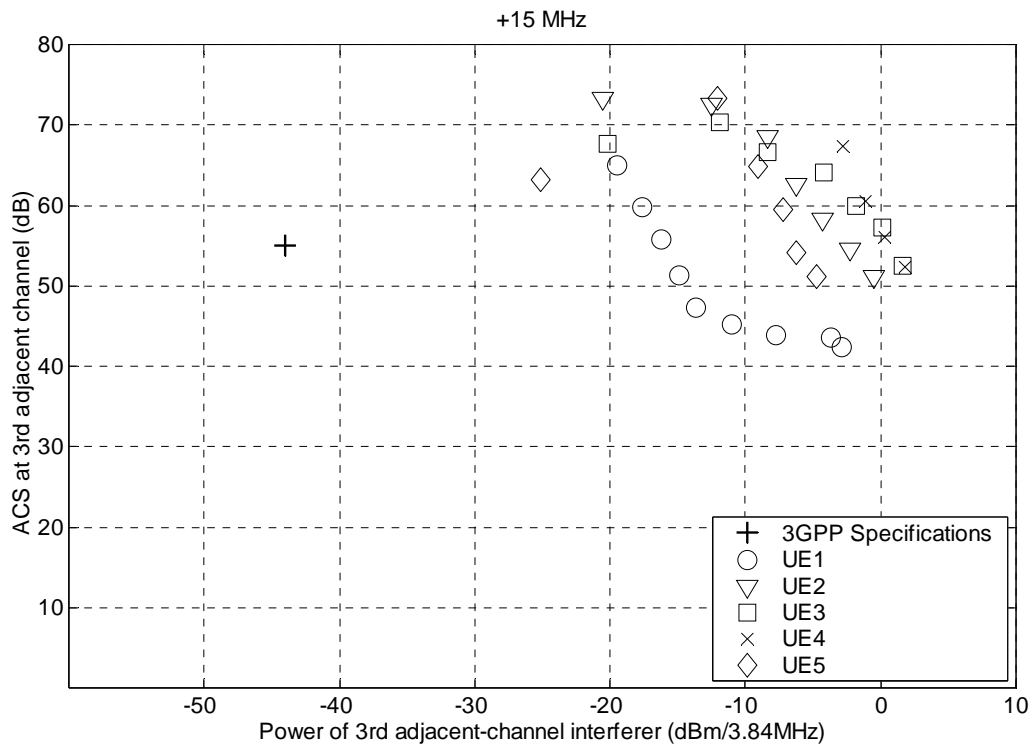
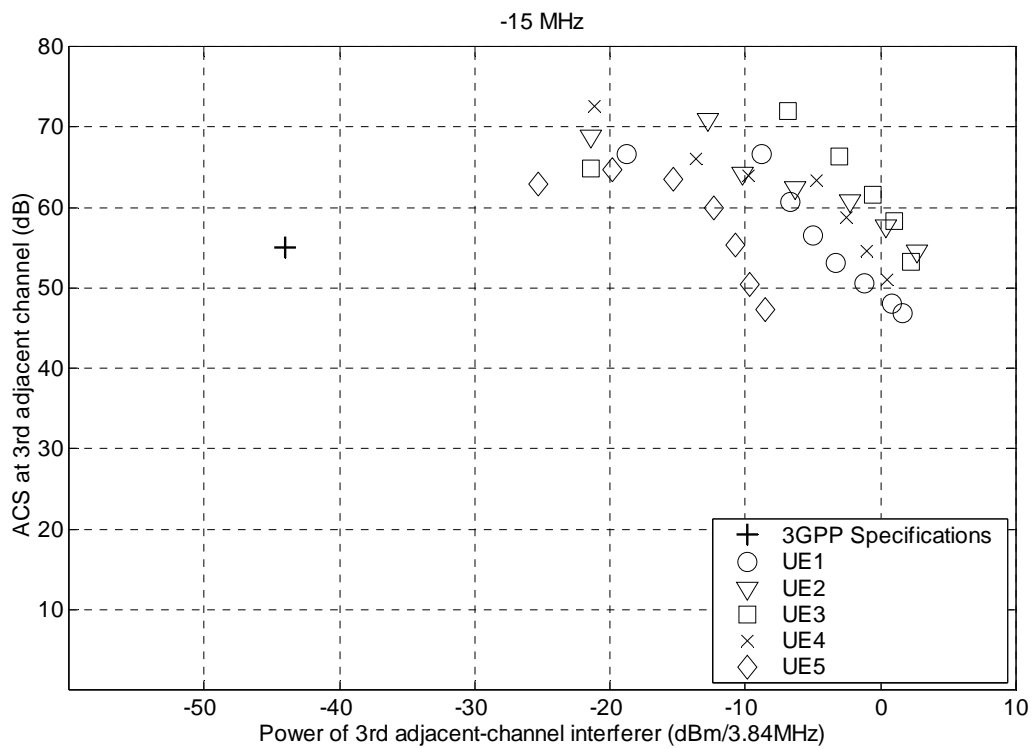


Figure 33: UE ACS at the 3rd adjacent channel (-15 MHz).



Measurements of UE receiver third-order inter-modulation performance

- A3.34 Figure 34 and Figure 35 show measurements at the UE of the received power, P_S , of a wanted downlink signal as a function of the received power, P_{AC} , associated with a first interferer received at the 2nd adjacent channel, and a second interferer received at the 4th adjacent channel, and for a constant bit-error probability of 10^{-3} .
- A3.35 Results are presented for five different UEs and for carrier-to-carrier frequency offsets of ± 10 and ± 20 MHz between the wanted signal and interferer. Also shown are the minimum requirements for the above parameters as specified in 3GPP TS 25.101.
- A3.36 The following observations can be made:
- As might be expected, every 10 dB increase in the interferer power results in a 30 dB increase in the wanted signal power in order to maintain a fixed bit-error probability.
 - When averaged across all tested UEs, the measurements indicate that the third-order inter-modulation performance of a UE receiver is around 15 dB better than the 3GPP minimum requirements.
 - When averaged across all tested UEs, the measurements suggest an interferer power of just below -30 dBm/(3.84 MHz) for a wanted signal power of -103.7 dBm/(3.84 MHz). This is to be compared with a 3GPP minimum requirement for an interferer power of -46 dBm/(3.84 MHz)⁴⁰ at a wanted signal power of -103.7 dBm/(3.84 MHz).
- A3.37 Based on the above observations, we have assumed a third-order inter-modulation reference adjacent-channel power, Π_{AC} , of -30 dBm in the derivation of the results presented in Section 4 of this document (as also described in Annex 1).

⁴⁰ 3GPP TS 25.101 specifies that the inter-modulation characteristics of a terminal station receiver should be such that the reception of two interferers, each at a level of -46 dBm and at frequency offsets of 10 and 20 MHz from the wanted carrier, should at most result in a 3 dB desensitisation with respect to the reference sensitivity performance. The reference sensitivity wanted signal power is -106.7 dBm/(3.84 MHz).

Figure 34: Measured variation of P_s versus P_{AC} for UEs in the presence of interferers at the 2nd and 4th (+10 and +20 MHz) adjacent channels and for a DL bit-error rate of 10^{-3} .

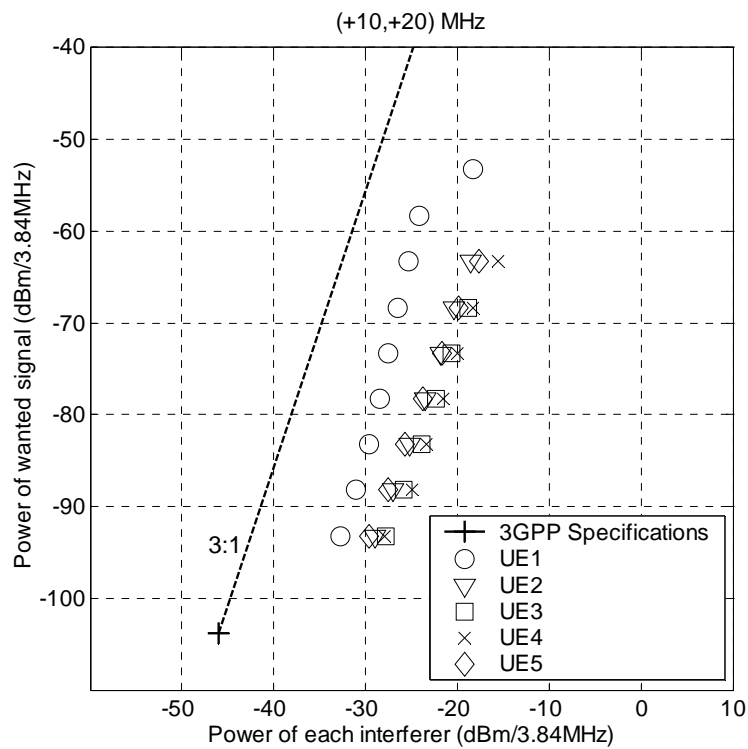
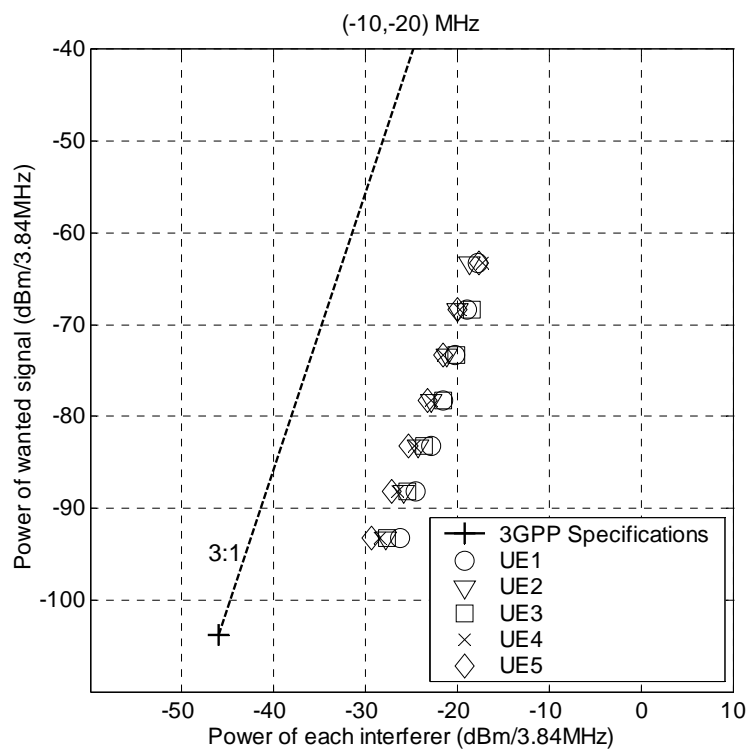


Figure 35: Measured variation of P_s versus P_{AC} for UEs in the presence of interferers at the 2nd and 4th (-10 and -20 MHz) adjacent channels and for a DL bit-error rate of 10^{-3} .



Conclusions

- A3.38 We have shown, based on measurements of frequency discrimination in UTRA-FDD UEs in the 2.1 GHz band, that terminal stations of the type which might be deployed in the 2.6 GHz band can be characterised by ACS values of up to 53, 65, and 70 dB in the presence of adjacent-channel interferers of up to -25 , -15 , and -15 dBm/(3.84 MHz) at the 1st, 2nd, and 3rd adjacent (5 MHz) blocks respectively.
- A3.39 The measurements also indicate that the 3GPP minimum requirements for ACS can be achieved in the presence of adjacent-channel interferers of up to -10 , 0 , and -5 dBm/(3.84 MHz) at the 1st, 2nd, and 3rd adjacent (5 MHz) blocks respectively.
- A3.40 Measurements finally indicate that the third-order inter-modulation performance of a UE receiver is typically around 15 dB better than the 3GPP minimum requirements.
- A3.41 Accordingly, we have assumed a) conservative ACS values of 53, 65, 65 and 65 dB at the 1st, 2nd, 3rd, and 4th adjacent blocks, b) a saturation interferer power threshold of -10 dBm, and c) an inter-modulation reference adjacent-channel power of -30 dBm, in the analysis presented in Section 4 of this document for the evaluation of the impact of terminal-to-terminal interference in the 2.6 GHz band.

